Balancing Fairness and Economic Impact: A Novel Approach to Rumor Mitigation in Social Networks

Jiajie Fu, Xueqin Chang, Xiangyu Ke, Lu Chen, Yunjun Gao
Zhejiang University
{jiajiefu,changxq,xiangyu.ke,luchen,gaoyj}@zju.edu.cn

ABSTRACT

The wild spread of negative information, e.g., rumors and disinformation, has been a major concern for social network platform owners. Existing research always try to curb the spread of rumors by maximizing the number of users influenced by truth. However, the algorithms designed for this purpose neither consider the individual-level economic losses caused by rumors nor account for the critical factor of fairness. To address these limitations, we propose a novel problem: the Fairness-aware Temporal Loss-based Rumor Mitigation (FAIR-TLRM) problem, which seeks to identify a truth spread set that minimizes the expected losses caused by rumors while satisfying fairness constraints. We first prove the FAIR-TLRM problem is NP-hard, monotone and non-submodular. Then, we propose a greedy-based dual-objective optimization algorithm, Fair-Greedy, to greedily select the truth spread users. Since computing mitigation reward of any truth spread set is #P-hard, we devise a scalable algorithm FWS-RM by employing group-aware weighted-RIS and sandwich technical to efficiently address the FAIR-TLRM problem. By employing FWS-RM, We conducted several explorations on how to make a balance between the losses caused by rumors and the fairness constraints and further propose a framework called Joint-Greedy. Compared with existing algorithms, FWS-RM reduces the economic losses stemming from rumors by an average of 2 times, improves fairness by up to 8 times, and runs 5× faster than baselines.

PVLDB Reference Format:
Jiajie Fu, Xueqin Chang, Xiangyu Ke, Lu Chen, Yunjun Gao. Balancing Fairness and Economic Impact: A Novel Approach to Rumor Mitigation in Social Networks. PVLDB, 14(1): XXX-XXX, 2023.
doi:XX.XX/XXX.XX

PVLDB Artifact Availability:
The source code, data, and/or other artifacts have been made available at https://github.com/FuJiaJie123/TLRM.

1 INTRODUCTION

Social networks have become key platforms for information dissemination, playing a critical role in applications such as recommendation systems [62], network monitoring [27], and viral marketing [11]. These applications have generated substantial revenue, contributing billions to the owners of these networks. However, the rapid growth of social networks has also facilitated the spread of harmful content, including rumors and disinformation [57], leading to significant financial losses. For instance, Velichety et al. found that false news can easily result in a loss of 2.11 million USD in equity value over a ten-day period on Twitter [55].

Existing approaches for rumor mitigation can be broadly divided into blocking-based methods [36, 47, 61] and clarification-based methods [33, 42, 45]. Blocking-based methods focus on removing user accounts or connections from networks to stop the spread of rumors, while clarification-based methods disseminate factual information to counteract rumors. However, banning user accounts or connections can significantly disrupt the network structure and raise ethical concerns [59]. Therefore, this paper adopts clarification-based methods to address rumor mitigation.

Recent studies show that positive user engagement is crucial for social network platforms, as their stock prices and advertising revenue are closely linked to user activity [41, 56]. However, the rapid spread of rumors on online social networks (OSNs) can significantly erode user trust, leading to a decline in engagement and, consequently, a drop in platform revenue [55]. Existing clarification-based methods primarily aim to reduce the number of users exposed to rumors, overlooking the economic impact of diminished engagement. In this work, we address this gap by using user engagement as a metric to assess the effect of rumors. Users with higher engagement levels pose greater potential losses to social network platforms, as they are more likely to reduce their activity after encountering rumors [10].

Additionally, existing research indicates that many rumors are often targeted at specific groups [32, 54]. For instance, a study conducted at the University of Texas at Austin[1] revealed that communities of color and diaspora populations are frequently the focus of online malign influence campaigns, particularly during elections and health crises. In 2021, for example, rumors related to COVID-19 spread rapidly among Latino and African American communities. This targeting undermines the healthy development of social networks [22, 26]. Despite these significant fairness concerns, current studies often fail to address them.

Building on the motivations discussed above, we revisit the rumor mitigation problem and introduce a novel approach called the Fairness-aware Temporal Loss-based Rumor Mitigation (FAIR-TLRM) problem. The objective of the ours is to identify a budget-limited truth seed set S_T, such that the expected losses caused by the rumor are minimized after S_T disseminates the truth, while improving the welfare for the least advantaged group until it reaches a pre-determined threshold. Practically, such group is often overlooked when pursuing for high loss reduction in RM (§ 6.1).

[1]https://mediaengagement.org/research/the-impact-of-disinformation-targeted-at-communities-of-color

Proceedings of the VLDB Endowment, Vol. 14, No. 1 ISSN 2150-8097.
doi:XX.XX/XXX.XX

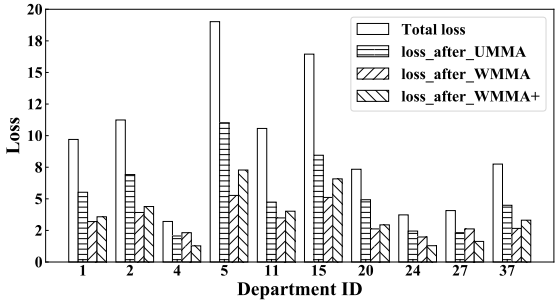

Figure 1: The loss of different departments. The "total loss" represents the initial loss within each department before any intervention. "Loss_after_UMMA" shows the loss after applying the UMMA algorithm, and similarly for "Loss_after_WMMA" and "Loss_after_WMMA+".

Case Study. To motivate our study, we conduct a case study on the real-world Email-EuAll social network [29], which captures email communication between users. Each user in this dataset is associated with a specific department based on her job occupation, forming a total of **42** groups. For the study, we randomly selected 10 nodes as rumor seeds and set the fairness parameter α to 0.9. Subsequently, a truth campaign comprising 50 was initiated to mitigate the spread of rumors and restore trust.

[Settings] We implement three simple greedy in the case study.[2] (1) Unweighted Rumor Mitigation Algorithm (UMMA): Selects the truth spread set without considering node weight; (2) Weighted Rumor Mitigation Algorithm (WMMA): Selects the truth spread set while accounting for node weight; and (3) WMMA+: Extends WMMA by introducing a fairness constraint. We then analyzed the results based on the losses and the number of influenced users across different departments. It's important to note that we only display results for departments where the total loss exceeds 0.2, as excluding departments below this threshold does not impact the overall analysis. To measure the effectiveness of the algorithms, we use the **save ratio**, calculated as the proportion of the initial loss mitigated by each algorithm.

[Economic Impact and Fairness] As illustrated in Figure 1, both the WMMA and WMMA+ algorithms achieved greater economic loss reduction than UMMA (i.e., lower bar; see Table 1 for detailed data). This demonstrates that traditional methods [6, 45], which focus solely on minimizing the number of affected users, fail to account for the varying economic value of different users.

However, both WMMA and UMMA struggled with significant fairness issues. For instance, in department 4, the save ratio for UMMA was only 34.78%, much lower compared to the 55.15% achieved in department 11. The fairness issue was even more pronounced for WMMA, where the save ratio in department 4 dropped to just 27.73%, compared to a high of 72.29% in department 5. This discrepancy stems from the fact that users with high engagement (i.e., larger node weights) tend to be clustered within the same group, which worsens the fairness imbalance. After applying the WMMA+ algorithm, the save ratio in department 4 improved to 60.12%. Even in department 37, which had the lowest save ratio, the percentage increased to 57.29%. As shown in Table 1, the sacrificed

[2]UMMA is the existing method mentioned in [6], WMMA+ is the algorithm we proposed in § 5.1 (i.e., Fair-Greedy).

Table 1: The loss after applying three algorithm

Metric \ Method	UMMA	WMMA	WMMA+
Total Loss	216.62	216.62	216.62
Loss After Algorithm	127.05	72.16	84.71
Save Ratio	41.35%	66.69%	60.89%

economic loss for ensuring fairness is minimal (reduced by less than 6% and is still much higher than the 41.35% of UMMA).

[Compatibility with Maximizing Affected User Count] We applied the three algorithms to the traditional rumor mitigation problem, which focuses on minimizing the number of users affected by rumors. Although the number of rumor-affected users is smaller after applying UMMA compared to WMMA and WMMA+ (i.e., slightly lower bar values in Figure 2), Table 2 demonstrate that the performance of WMMA and WMMA+ is very close to that of UMMA, achieving nearly 96% of its effectiveness. This demonstrates that our algorithms perform well not only on the Fair-TLRM problem but also on the traditional RM problem.

Table 2: The influence after applying three algorithm

Metric \ Method	UMMA	WMMA	WMMA+
Total Influence	459.28	459.28	459.28
Influence After Algorithm	167.23	175.45	178.57
Save Ratio	63.59%	61.79%	61.12%

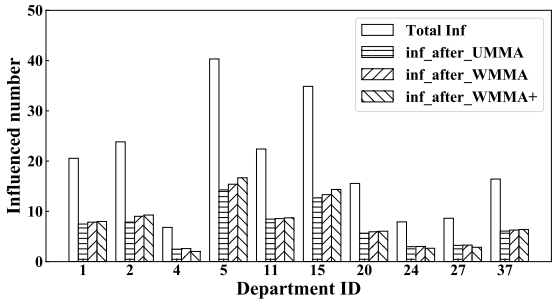

Figure 2: The inf of different groups

Challenges and Our Contributions. To the best of our knowledge, we are the first to study the FAIR-TLRM problem, which minimizes the losses caused by rumor considering the fairness issue. We prove that the FAIR-TLRM problem is **NP**-hard and it is #P-hard to compute the loss reduction brought by truth set (i.e., **NP**-hardness as proved in Section 4). A basic idea is to maximize the users believed in truth with the presence of S_T [6]. However, such method neither considers the different individual loss reduction resulted from *successful rescue*, nor does it take the constraint of fairness into considerations. To this end, we propose *Fair-Greedy*, a greedy-based dual-objective optimization approach that consists of two stages to choose the truth seed set. As shown in Table 1, compare to existing methods [6, 45] that simply maximize the number of users reached by truth, *Fair-Greedy* can increase the save ratio by 19.54%, (i.e., from 41.35% to 60.89%).

However, *Fair-Greedy* suffers from severe time cost, this motivates us to propose an efficient and effective approach to tackle

this issue. Many recent works adopt Reverse Influence Sampling (RIS) [4, 51, 52] to accelerate the computation of influence spread of IM-Related problems. However, the RIS method cannot be directly applied to our problem since it does not take into account the concept of groups and loss weights. Therefore, we first designed a new RR-Set generation method GRASS. Then, based on GRASS, we propose *FWS-RM*, a solution that not only solves the problem effectively, but also greatly decreases the time complexity of *Fair-Greedy*. Additionally, through several case studies, we found that using FWS-RM with excessive consideration of fairness may lead to poor performance of the algorithm. Thus, we conducted a detailed analysis and proposed a novel framework *Joint-Greedy* for better algorithm-performing.

Contributions and Roadmap.

- To our best knowledge, we are the first to formulate the problem of *Fair-TLRM*, which considers the losses caused by rumor and the fairness constraint (Section 3). We prove that *Fair-TLRM* is **NP**-hard, non-submodular and it is #P-hard to compute the loss reduction brought by any truth seed set (Section 4).
- We first propose a greedy-based dual-objective optimization algorithm *Fair-Greedy*. Then, based on a novel group-aware weighted-RIS and sandwich approximation technique, we devise *FWS-RM* that significantly improves the efficiency while ensuring a $(1 - 1/e - \epsilon)$-approximation guarantee under our bounding functions (Section 5).
- We conduct several meaningful case studies and give insight advises on making a balance between the loss reduction and the maintain fairness and propose a framework *Joint-Greedy* to further improve the algorithm performance. (Section 6).
- We conduct thorough experimental evaluations on five real-world social networks. The results demonstrate that our algorithm is effective and efficient (Section 7).

2 RELATED WORK

Influence Maximization. The Influence Maximization (IM) problem was firstly formulated as a discrete optimization problem by Kempe et al. [24] where they introduced two fundamental propagation models, i.e., the IC and LT models. They demonstrated that the IM problem is **NP**-hard under both models and proposed a greedy algorithm with $(1 - 1/e)$-approximation. To estimate influence spread from a seed set, they employed Monte Carlo simulations, which was later proved #P-Hard to exactly compute [8]. Afterwards, numerous solutions were devised for efficiently tackle the IM problem [18, 20, 50–52]. Most of these approaches rely on reverse influence sampling methods [4]. Additionally, various variants of IM have been explored [7, 9, 23, 44].

Rumor Mitigation. Extensive research has been conducted on the *Rumor Mitigation* (RM) problem, which aims to limit the spread of rumor in social networks. Budak et al. [6] first introduced this problem under the IC model, followed by Fan et al. [12] under the LT model. Since then, substantial follow-up research has sought efficient methods to address RM and its variant [38, 43, 53].

In addition to launching a truth campaign as mentioned above, blocking strategies have emerged as another primary approach to address the RM problem [37, 46, 58]. Recently, Xie et al. first applied the dominator tree structure to efficiently compute the decrease of the expected spread of all candidate blockers [61].

Table 3: Frequently used notation

Notation	Description
T, F, S_T, S_F	The truth and rumor campaigns, and their respective seed sets
τ	The activation window, i.e., the time a user takes to decide after first receiving a message
α	The fairness threshold: the solution must achieve at least an α-fraction of the optimal fairness score
C, C_i, c	The disjoint group affiliation of nodes, i.e., $C = \{C_0, C_1, ..., C_c\}$, C_i represents the i^{th} group among the affiliation and c is the total number of groups
d_e^F, d_e^T	The delay for rumor and truth propagation on edge e
t_e^F, t_e^T	The timestamp that v is reached by F or T
$\mathbb{R}(S_T)$	The loss reduction results from the truth seed set S_T, i.e., $\mathbb{L}(G, S_F, S_T) - L(G, S_F, \emptyset)$
X, X'	X is a fixed possible world, and X' is the corresponding revised possible world with all delays for campaign T set to 1
MAS_X	The set of nodes affected by the rumor in X
$r(S_T \to v)$	The loss reduction (or reward gain) to v due to truth set S_T. $r_X(S_T \to v)$ denotes such reduction in a specific possible world X
$\mathcal{P}_v^T, \mathcal{P}_v^F$	The set of the paths from the truth (resp. rumor) set to user v
$a(\mathcal{P}_v^T, \mathcal{P}_v^F)$	An indicator that takes 1 if there are common edges in $\mathcal{P}_v^T$ and $\mathcal{P}_v^F$; otherwise, it equals 0

Nevertheless, few of these works consider the fact that the propagation speed of truth and rumor differs. The recently proposed TCIC model [42] addresses this gap by accounting for this difference, but the focus is not on reducing economic losses yet. Moreover, existing studies fail to provide methods for assessing the individual financial losses incurred by social platforms when users encounter rumors. Additionally, they do not account for fairness considerations.

In this paper, we address the novel problem of minimizing rumor-induced losses in OSNs while incorporating fairness (Fair-TLRM). We propose an efficient approach that utilizes a group-aware weighted RIS approach combined with a sandwich technique, providing valuable insights into balancing the trade-off between economic losses from rumors and fairness constraints.

3 PRELIMINARIES

In this section, we introduce the TCIC model (§ 3.1) and present various methods for measuring individual user losses when influenced by rumors (§ 3.2). Building on this foundation, we formally define the Fairness-aware Temporal Loss-based Rumor Mitigation (Fair-TLRM) problem (§ 3.3).

3.1 The TCIC Model

Consider a directed graph $G = (V, E, p)$, where V and $E \subseteq V \times V$ represent the sets of vertices and edges, respectively. Let $|V| = n$ and $|E| = m$. Each edge $e = (u, v)$ is associated with an influence weight $p_{u,v} \in [0,1]$, which quantifies the impact strength of u on v.

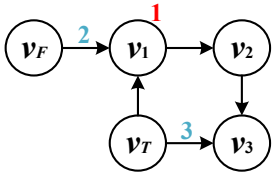

Figure 3: The propagation process under TCIC model

The Temporal Competitive Independent Cascade (TCIC) model depicts a diffusion process where two mutually exclusive campaigns, rumor (F) and truth (T), vie for propagation [42]. Unlike the traditional CIC [2, 9] and IC [24] models, which assume uniform propagation rates, TCIC introduce a a key distinction: a *meeting delay* to account for varying propagation speeds of different types of information[3]. Additionally, TCIC incorporates the concept of an *activation window (AW)*, a period during which users contemplate which information to adopt [16]. If both campaigns reach a user in this window, a *proportional tie-breaking* dictates her decision.

The propagation dynamics of the TCIC model are outlined as follows: **(1)** Seeds S_F for rumor and S_T for truth are activated at timestamp 0, while other nodes remain inactive; **(2)** Each newly activated node has one chance to influence its inactive neighbors after a specified *meeting delay*, with the likelihood of success determined by the edge's influence probability. **(3)** Once activated, a node enters an *activation window*, after which it adopts either F, T, or uses *tie-breaking rules*[4] if influenced by both. After adoption, we assume the user remains committed to their decision. **(4)** Propagation continues until no further nodes can be activated.

Example 1. *In Figure 3, v_F is the rumor seed and v_T is the truth seed. All edges share a same propagation probability of* 1*. The blue numbers on the edges represent the meeting delays of truth. We assume a constant delay of 1 for rumor. The red number beside the node represents the activation window, with unspecified AW lengths set to 0*[5]*. We exemplify the influence propagation as follows:*

- *$t = 0$, node v_F and v_T activate.*
- *$t = 1$, rumor from v_F reaches v_1, opening v_1's AW.*
- *$t = 2$, truth from v_T reaches v_1 at the end of its AW. Following the tie-breaking rule, v_1 adopts F or T with equal probability. Let us assume v_1 adopts F.*
- *$t = 3$, v_3 is influenced by v_T and v_2 by v_1. As both AWs are 0, v_3 adopts T while v_2 adopts F, and the propagation concludes.*

The rumor mitigation reward only accounts for nodes that would have adopted the rumor in the absence of the truth set but switch to adopting the truth once the truth set is introduced. These nodes are considered to be "successfully rescued". A similar approach is outlined in [6, 42].

3.2 Individual user losses measurement method

In this section, we detail two distinct methods for assessing user engagement. These methods quantify the impact of being affected by rumors, relying on either network topology or user historical behavior data. In addition, we keep another basic method of assigning random weights for experimental purposes in later sections.

- ***Topology-based:*** Lurker ranking methodologies [48, 49] assign users scores that reflect their level of activity within a social network, especially the passive ones. The intuition is that, in social networks, a user's in-degree often represents her information reception, while the out-degree signifies her contribution to information sharing, both of which provide a robust indicator of user activity. The user engagement score based on network topology is calculated as follows: the assumption is that a node v with infinite in/out-degree ratio is trivially regarded as a lurker, $dx+(1-d)y$ and $w_{in}(v)(1+w_{out}(v))$ come from the combination of alpha-centrality [3] and PageRank [5]. For more details, please refer to [49]:

$$w(v) = d[w_{in}(v)(1 + w_{out}(v))] + (1 - d)p(v) \tag{1}$$

  where $w_{in}(v)$ is the in-neighbors-driven score function, the idea behind it is that the strength of v's lurking status is proportional to the influential status of the v's in-neighbors, and it's further enhanced by including a factor that is inversely proportional to the v's out-degree. And $p(v)$ is a personalized value, which is set to $1/|V|$ by default:

$$w_{in}(v) = \frac{1}{out(v)} \sum_{u \in N^{in}(v)} \frac{out(u)}{in(u)} w(u) \tag{2}$$

  and $w_{out}(v)$ is the out-neighbors-driven score function, it follows the principle of *Non-authoritativeness of the information produced*, i.e., the strength of v's lurking status is proportional to the lurking status of the v's out-neighbors:

$$w_{out}(v) = \frac{in(v)}{\sum_{u \in N^{out}(v)} in(u)} \sum_{u \in N^{out}(v)} \frac{in(u)}{out(u)} w(u) \tag{3}$$

  This lurker ranking score is then logarithmically transformed and normalized to obtain a value between $[0, 1]$, representing the users' silence weights. To derive the user's node weight (i.e., active weight), we subtract the silence weight from 1.
- ***Historical-data-based:*** A user's historical behavior data is often the most direct indicator of her engagement level, such as app usage time, purchase records, or review counts. The most widely-used logarithmic normalization method [40] is given as below:

$$w(v) = \frac{log(1 + count(v))}{log(1 + max_{u \in V}\, count(u))} \tag{4}$$

  Where V is the vertex set in social network G and $count(v)$ could be any frequency-based historical data associated with user v.

3.3 Problem Definition

Given a known rumor seed set S_F, our goal is to identify a truth seed set S_T that minimizes the losses caused by the rumor while maintaining a desired level of fairness. Specifically, we aim to save the nodes that would otherwise adopt the rumor in the absence of S_T, maximizing the *total losses* (i.e., node weights) of the saved nodes, all within the fairness constraint.

Definition 1. (Loss Measure Function). *Given a graph G, a rumor seed set S_F and a truth seed set S_T, the loss measure function*

[3]Rumors typically propagate faster than truth by an average factor of 6× [57].
[4]TCIC usually applies a weighted random choice policy based on the number of activated neighbors. Specifically, a node u adopts rumor F with probability $p_F(u) = |N_F^-(u)|/|N^-(u)|$, where $|N_F^-(u)|$ is the number of neighbors who propagated F, and $|N^-(u)|$ is the total number of neighbors exposed to either F or T. The same logic applies to the truth campaign.
[5]Unless otherwise specified, in this work we set the activation window to 0 for simplicity, though our algorithm is applicable to all possible values.

$\mathbb{L}(G, S_F, S_T)$ *represents the expected losses caused by rumor on graph* G *under* TCIC *model, formally,*

$$\mathbb{L}(G, S_F, S_T) = \sum_{v \in MAS} w(v) \tag{5}$$

where MAS represents the nodes affected by rumors.

When given the specific group C_i, the expected losses on the i^{th} group of G can be written as $\mathbb{L}_i(G, C_i, S_F, S_T)$.

Definition 2. (Maxmin Fairness). *Given a graph* G*, a rumor seed set* S_F*, a budget* b*, and a group division* C *of nodes in* G*, the Maxmin-Fairness of* G *is:*

$$opt(G, S_F, b, C) = \max_{\substack{S_T \subseteq V \setminus S_F, \\ |S_T| \le b}} \min_{C_i \in C} \frac{\mathbb{L}_i(G, C_i, S_F, \emptyset) - \mathbb{L}_i(G, C_i, S_F, S_T)}{\mathbb{L}_i(G, C_i, S_F, \emptyset)}$$

Unlike *Equality Fairness* and *Diversity Fairness* [13] that often struggle to accommodate balanced outcomes, the *Maximin Fairness* aligns with John Rawls' well-known philosophical "Theory of Justice" [39]: *Societal systems should be structured to maximize the welfare of the least advantaged group.* In social analysis, policies often aim to reduce inequality by improving conditions for the worst-off rather than just ensuring equal treatment across all groups. Maximin fairness prioritizes the most affected individuals (e.g., those most seriously impacted by rumors), making it a straightforward yet powerful tool for evaluating and promoting equitable interventions, such as the dissemination of factual information.

Problem 1. (Fair-TLRM). *Given a social graph* G*, a rumor seed set* S_F*, a budget* b*, and a threshold* α*. The Fairness-aware Temporal Loss-based Rumor Mitigation (Fair-TLRM) problem finds a truth spread set* S_{T^*} *of at most* b *nodes that minimizes the expected losses while achieving at least* α *of the maxmin fairness. Formally:*

$$S_{T^*} := \arg \min_{\substack{S_T \subseteq (V \setminus S_F), \\ |S_T| \le b}} \mathbb{L}(G, S_F, S_T)$$

$$s.t. \ \min_i \frac{\mathbb{L}_i(G, C_i, S_F, \emptyset) - \mathbb{L}_i(G, C_i, S_F, S_T)}{\mathbb{L}_i(G, C_i, S_F, \emptyset)} \ge \alpha * opt$$

4 PROBLEM CHARACTERISTICS

In this section, we analyze the computational complexity and mathematical properties of the Fair-TLRM problem. First, we establish the **NP**-hardness of the Fair-TLRM problem. Then, we prove that the Fair-TLRM is both *monotone* and *non-submodular*.

NP-Hardness. The Influence Minimization (IM) problem under the CIC model has been proven to be **NP**-hard [6]. The CIC-based IM can be viewed as a special case of Fair-TLRM problem, where the meeting delay $m(u, v) = 1$ for all nodes is set to 1, all node weights are equal 1, the activation window (AW) is zero, truth-dominant tie-breaking[6] is applied, and the fairness threshold α is set to 0. Given these conditions, the Fair-TLRM problem inherits the **NP**-hardness of the IM problem under the CIC model.

Monotonicity. Our Fair-TLRM problem remains *monotonically non-increasing* under TCIC model, as shown in the theorem below.

[6]In truth-dominant tie-breaking, when both campaigns reach a node, the node always chooses the truth, which is a simplified form of proportional tie-breaking mentioned in 3.1 and does not affect the NP-hardness.

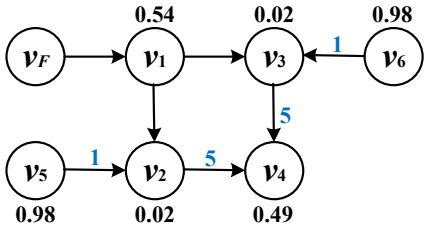

Figure 4: Example to proof the non-submodularity

Theorem 1. *Given a graph* G *and a rumor seed set* S_F*, the function* $\mathbb{L}(G, S_F, S_T)$ *is monotonically non-increasing under the* TCIC *model.*

Proof. Let S_z and $S_{z'}$ be two truth seed sets such that $S_z \subseteq S_{z'} \subseteq (V \setminus S_F)$. Since adding more truth seeds can only reduce the number of nodes influenced by rumors, we must have $\mathbb{L}(G, S_F, S_{z'}) \le \mathbb{L}(G, S_F, S_z)$. Furthermore, if S_z has satisfied the fairness constraint, adding any node $v \in S_{z'} \setminus S_z$ to S_z will not violate the fairness constraint, since the group with the minimum gain has already met the fairness requirement. This completes the proof. □

Non-Submodularity. We illustrate the non-submodularity of the Fair-TLRM problem using a counterexample.

Theorem 2. *The Fair-TLRM problem is non-submodular under the* TCIC *model.*

Proof. Consider the graph in Figure 4, where v_F represents the rumor node. Assume the rumor propagation delay d_e^F takes 1 for each edge, while those for truth d_e^T are given by the **blue** numbers. The weight beside each node is calculated using the Lurker ranking algorithm [49]. The fairness constraint parameter α is set to 0, i.e., any truth seed set simply satisfies the fairness constraint.

$\{v_2, v_3, v_4\}$ are originally affected by the rumor. Consider two truth seed sets: $A = \emptyset \subseteq B = \{v5\}$. Truth seed v_5 can reach two victims v_2 and v_4. v_2 can be successfully rescued as $t^T_{v_2} = 1 < t^F_{v_2} = 2$. For v_4, there still exists a faster rumor pathway $v_F \to v_1 \to v_3 \to v_4$, leading to $t^F_{v_4} = 3 < t^T_{v_4} = 6$. Therefore, v_4 cannot be saved and the cost reduction is only $\mathbb{R}(B) = w(v_2) = 0.02$.

Now, consider adding v_6 to both sets: as the toy graph is symmetric, we can easily obtain $\mathbb{R}(A \cup \{u\}) = w(v_3) = 0.02$. Moreover, securing v_3 cuts off the aforementioned rumor pathway to v_4, leading to a significant increase in loss reduction, i.e., $\mathbb{R}(B \cup \{u\}) = w(v_2) + w(v_3) + w(v_4) = 0.02 + 0.02 + 0.49 = 0.53$. Hence, we have $\mathbb{R}(B \cup \{u\}) - \mathbb{R}(B) > \mathbb{R}(A \cup \{u\}) - \mathbb{R}(A)$ and $A \subseteq B$, indicating the non-submodularity of our Fair-TLRM problem. □

Sandwich Approximation. Sandwich approximation method [31] is a well-established approach to provide a data-dependent and quality-bounded solution to non-submodular problems (Lemma 1). Challenges lie in devising a pair of submodular lower ($\underline{\mathbb{R}}$) and upper bounds ($\overline{\mathbb{R}}$) respectively. Next, we present our design and demonstrate the practicality later in § 7.2.

Lemma 1 ([31]). $\mathbb{R}(S_T) \ge \beta \cdot (1 - 1/e) \cdot \mathbb{R}(S^o_T)$*, where* $\beta = \max\{\frac{\mathbb{R}(S^U_T)}{\overline{\mathbb{R}}(S^U_T)}, \frac{\underline{\mathbb{R}}(S^o_T)}{\mathbb{R}(S^o_T)}\}$*,* S^o_T *is the optimal solution and* S^U_T *is the solution obtaining by upper bounding function.*

We adopt the *Possible World* semantic [24] to facilitate the illustration. Given a uncertain graph G, a possible world $X = (V, E_X)$

is generated by randomly removing each edge $e = (u, v)$ in G with $1 - p(u, v)$ probability. The probability of any possible world X occurring is $P(X) = \prod_{(u,v)\in E_X} p_{u,v} \prod_{(u,v)\in E\setminus E_X} (1 - p_{u,v})$. This yields 2^m distinct possible worlds, denoted as $\mathcal{X}$. The meeting delay on each edge in E_X and the activation time of users are assumed to be pre-determined: The former is sampled through the geometric distribution separately for F and M while the latter can be set to zero for simplicity in the discussion below.

Lower Bound. In any fixed possible world X, the loss reduction for a node v, denoted by $r_X(S_T \to v)$, depends on whether S_T rescues v. It takes either $p_T(v) \cdot w(v)$ or 0, where $p_T(v) = 1$ if T rescues v without proportional tie breaking, or $p_T(v)$ is the probability that T wins the tie-breaking when both campaigns reach v. The expected loss reduction for v across all possible worlds, denoted by $r(S_T \to v)$, is the weighted sum over all possible worlds, i.e., $r(S_T \to v) = \sum_{X\in\mathcal{X}} Pr(X) \cdot r_X(S_T \to v)$. Hence, we define the lower bound $\underline{\mathbb{R}}(S_T)$ by considering only the nodes in S_T that provide the largest loss reduction to each v and summing these values for all v. Since the loss reduction from the entire truth seed set S_T is evidently not smaller than that from any individual node in S_T, intuitively, we have $\underline{\mathbb{R}}(S_T) \le \mathbb{R}(S_T) = \sum_v r(S_T \to v)$.

Lemma 2. *$\underline{\mathbb{R}}(S_T) = \sum_v \underline{r}(S_T \to v)$ is a submodular lower bound of $\mathbb{R}(S_T)$, where $\underline{r}(S_T \to v) = max_{u\in S_T} r(\{u\} \to v)$.*

Proof: In any possible world X, it is sufficient to demonstrate submodularity for each affected users, i.e., $v \in MAS_X$, due to closed property of summing submodular functions [15]. Denote $\underline{r_X}(S_T \to v) = max_{u\in S_T} r_X(\{u\} \to v)$. Consider any node $v \in MAS_X$ that satisfies the following condition:

$$r_X(B \cup \{w\} \to v) > r_X(B \to v) \tag{6}$$

where B is a truth set and $w \in V\setminus(B \cup S_F)$. To satisfy Inequation 6, the following two cases must occur:

Case(i): v is influenced by F under B, but influenced by T under $B \cup \{w\}$ without a tie-breaking. Since we only consider the node that brings the max loss reduction in T, under B, $t_v^F < t_v^T$, and under $B \cup \{w\}$, $t_v^T < t_v^F$, the shortest path from $B \cup \{w\}$ to v must begin with w; otherwise, it contradicts Equation 6. Therefore, w contributes to the loss reduction.

Case(ii): v is influenced by F under B, but influenced by T under $B \cup \{w\}$ with a tie-breaking. If F and T arrive at v simultaneously, the probability of T winning the tie-breaking increases if more of v's in-neighbors adopt T. Let N_B^+ denote the number of v's in-neighbors that adopt T under B. To satisfy Equation 6, under B, $t_v^F \le t_v^T$, and under $B \cup \{w\}$, $t_v^T = t_v^F$ and $N_{B\cup\{w\}}^+ > N_B^+$. The shortest path from $B \cup \{w\}$ to v's in-neighbors must begin with w; otherwise, it contradicts Equation 6. Therefore, w contributes to the loss reduction.

From the above two cases, we could conclude that $\underline{r_X}(B\cup\{w\} \to v) = \underline{r_X}(\{w\} \to v)$, since node w is solely responsible for the increase in loss reduction achieved at v. Let $A \subseteq B$, similar to the situation of B, we can get $\underline{r_X}(A \cup \{w\} \to v) = \underline{r_X}(\{w\} \to v) = \underline{r_X}(B \cup \{w\} \to v)$. Besides, due to the monotonicity of $\underline{r}$, it must satisfy that $\underline{r_X}(A \to v) \le \underline{r_X}(B \to v)$, therefore, $\underline{r_X}(A \cup \{w\} \to v) - \underline{r_X}(A \to v) \ge \underline{r_X}(B\cup\{w\} \to v) - \underline{r_X}(B \to v)$. Since $\underline{r}(S_T \to v)$ is the weighed aggregation of $\underline{r_X}(S_T \to v)$ and $\underline{\mathbb{R}}$ is the linear aggregation of $\underline{r}$, thus $\underline{\mathbb{R}}$ is also submodular, the proof ends. □

Uppper Bound. Under TCIC model, the propagation of truth typically lags behind the rumor. To adjust the upper bound function, we reduce all truth meeting delays to 1, making $d_e^F = d_e^T$ for every e in graph G. We denote such revised possible world as X'. This faster truth spread allows truth to reach rumor-affected nodes sooner, increasing the potential loss reduction. For the bounding function $\overline{\mathbb{R}}$, similar to the lower bound, we only consider the node in S_T that offers the greatest loss reduction for each v. However, with proportional tie-breaking, focusing on a single node may decrease the value of $r_X(S_T \to v)$, since $r_X(S_T \to v) = p_T(v) \cdot w(v)$. Under this situation $p_T(v) = N_u^+ \le N_{S_T}^+$, lowering $p_T(v)$. To counter this, we revise the loss reduction function to $r^*(\cdot)$, where the loss reduction for v always equals $w(v)$ when it encounters a tie-breaking, regardless of which side v ultimately adopts.

Lemma 3. *Denote $\overline{r}_X(S_T \to v) = max_{u\in S_T} r^*_{X'}(\{u\} \to v)$ where $r^*_X(S_T \to v)$ is defined as follows:*

$$r^*_X(S_T \to v) = \begin{cases} 0 & \text{if } v \text{ is only reached by } S_F \\ w(v) & \text{otherwise.} \end{cases} \tag{7}$$

$\overline{\mathbb{R}}(S_T) = \sum_v \overline{r}(S_T \to v) = \sum_v \sum_{X\in\mathcal{X}} Pr(X) \cdot \overline{r}_X(S_T \to v)$ is submodular upper bound of $\mathbb{R}(S_T)$.

Proof: In any modified possible world X', there exist two cases: **(i)** v **is reached by truth earlier** under $B \cup \{w\}$, meaning v is still influenced by the rumor with truth set B but switches to truth under $B\cup\{w\}$. Thus, the shortest path to v must contain w; adding w helps reduce the loss for v. **(ii)** v **is contested by both rumor and truth** under $B \cup \{w\}$, that is, v is still influenced by the rumor under truth set B, but compete with truth under $B \cup \{w\}$. By modifying r to r^*, the loss reduction is always $w(v)$, regardless of the tie-breaking. In this case, the shortest path to v also begins with w. In both scenarios, w is responsible for reducing the loss at v. By monotonicity and aggregation over possible worlds, the loss reduction function $\overline{\mathbb{R}}(S_T)$ is submodular. □

Tighten the Upper Bound. Consider Figure 4, where neither v_5 nor v_6 alone can act as a truth seed to rescue v_4, but together they can. We call this *combination effect*, which arises because their paths to v_4 cannot block (i.e., *intersect* with) all the shortest paths from S_F to v_4 individually [7]. We introduce a indicator function a to determine whether the paths from S_F and S_T to node v intersect; if no overlap exist, $a(\mathcal{P}_v^T, \mathcal{P}_v^F) = 0$. When this happens, $r_X(S_T \to v) = max_{u\in S_T} r_X(\{u\} \to v)$. To improve the tightness of our lower bound, we revise $\overline{r}_X(S_T \to v)$ as follows:

$$\overline{r}_X(S_T \to v) = \begin{cases} max_{u\in S_T} r_X(\{u\} \to v) & \text{if } a(\mathcal{P}_v^T, \mathcal{P}_v^F) = 0 \\ max_{u\in S_T} r^*_{X'}(\{u\} \to v) & \text{otherwise.} \end{cases} \tag{8}$$

Proof: When $a(\mathcal{P}_v^T, \mathcal{P}_v^F) = 0$, which means there is no overlapped path from S_T and S_F to v. This implies that $r_X(S_T \to v) = max_{u\in S_T} r_X(\{u\} \to v)$. By modifying the reduction function and changing tie-breaking to the truth-dominant one, we obtain:

$$\overline{r}_X(S_T \to v) = \begin{cases} max_{u\in S_T} r'_X(\{u\} \to v) & \text{if } a(\mathcal{P}_v^T, \mathcal{P}_v^F) = 0 \\ max_{u\in S_T} r'_{X'}(\{u\} \to v) & \text{otherwise.} \end{cases} \tag{9}$$

[7] In aforementioned upper bound, we have consider the case of establishing even shorter path for truth.

Here, r' indicates the propagation follows a truth-dominant policy. It can be proved that $\bar{r}_X(S_T \rightarrow v)$ under (9) is submodularHowever, after removing all MLs, even without truth-dominance, the reduction we gain still forms an upper bound. The reason is that the *combination effect* comes from the meeting delay of truth, consider the graph in Figure 4, after removing all the MLs, v_5 itself can "save" v_4 without the help of v_6. Due to the fact that multiple nodes in S_T and S_F may arrive at v at the same time, with the existence of *proportional tie-breaking*, only consider the node with the maximum reduction is wrong, the reason is that if the meeting delay of truth is the same as rumor, then only consider the node u with maximum reduction will decrease the reduction at the node v who may encounter a tie-breaking with $N^+_{S_T} > N^+_u$. Therefore, we modify r to r^*. Now consider the graph in Figure 5[8] where $a(\mathcal{P}^T_v, \mathcal{P}^F_v) = 1$ and there exists a special case of tie-breaking: with $\{v_2\}$ as the truth set, the paths for rumor set $\{v_1\}$ to reach $\{v_3, v_6 ... v_7\}$ overlap with that of $\{v2\}$ to these nodes (the overlapped node is v_5, and there is a tie-breaking on v_5 – truth and rumor both reach v_5 at $t = 1$), by switching the r to r^*, the loss reduction of v_5 is always $w(v_5)$ no matter v_5 finally adopts which side, increasing the expected loss reduction. This observation justifies modifying the $\bar{r}_X(S_T \rightarrow v)$ to:

$$\bar{r}_X(S_T \rightarrow v) = \begin{cases} max_{u \in S_T} r_X(\{u\} \rightarrow v) & \text{if } a(\mathcal{P}^T_v, \mathcal{P}^F_v) = 0 \\ max_{u \in S_T} r^*_{X'}(\{u\} \rightarrow v) & \text{otherwise.} \end{cases} \quad (10)$$

Fix a possible world X, in order to demonstrate sub-modularity, it is sufficient to prove submodularity for each $v \in MAS_X$ by leveraging the closed property of submodular functions [15]. Consider a truth set B and a node $w \in V \setminus (S_F \cup B)$:

When $a(\mathcal{P}^T_v, \mathcal{P}^F_v) = 0$, in order to satisfy (6), the loss reduction at v must increase with the inclusion of node w. Consider the following two cases: (i) v is switching to adopt T under $B \cup \{w\}$ w/o tie-breaking and (ii) v believed in T under $B \cup \{w\}$ w/ tie-breaking.

Case(i): If v is influenced by F under B, but influenced by T under $B \cup \{w\}$ without a tie-breaking, for v to satisfy Inequality 6, under B, $t^F_v < t^T_v$, and under $B \cup \{w\}$, $t^T_v < t^F_v$. Therefore, the shortest path from $B \cup \{w\}$ to v must begin with w; otherwise, it contradicts the condition. w contributes to the reduction.

Case(ii): If v is influenced by F under B, but by T under $B \cup \{w\}$ with a tie-breaking, when F and T arrived at v simultaneously. The probability of winning a tie-breaking increases if more of v's in-neighbors adopt T. To satisfy (6), $t^F_v \leq t^T_v$ under B, and $t^T_v = t^F_v$ and $N^+_{B \cup \{w\}} > N^+_B$ under $B \cup \{w\}$. Hence, the shortest path from $B \cup \{w\}$ to v's in-neighbors must begin with w, otherwise it contradicts the condition. Therefore, w also contributes to the reduction.

When $a(\mathcal{P}^T_v, \mathcal{P}^F_v) = 1$, in order to satisfy (6), the loss reduction at v must increase with the inclusion of node w. Consider the following two cases: (i) v is not reached by F under $B \cup \{w\}$ and (ii) v is reached by F under $B \cup \{w\}$.

Case(i): Since v is not reached by F under $B \cup \{w\}$, e.g., truth reached v earlier, it must be the situation that under B, $t^F_v < t^T_v$, and under $B \cup \{w\}$, $t^T_v < t^F_v$. Therefore, the shortest path from $B \cup \{w\}$ to v must begin with w; otherwise, it contradicts the condition. w contributes to the loss reduction.

[8]The number beside the node is its node weight, the blue number represents the MLs of truth, MLs not shown are 1, the red number over the edge is the influence probability, default set is 1.

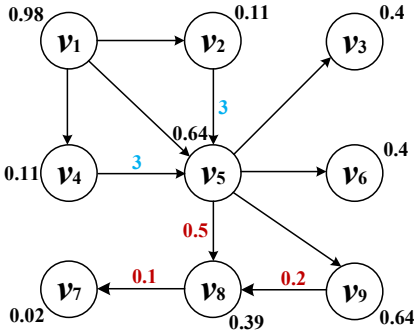

Figure 5: Upper bound sketch graph

Case(ii): By modifying r to r^*, even F and T arrived at v simultaneously, the obtained loss reduction is $w(v)$ regardless of the tie-breaking. To satisfy (6), $t^F_v < t^T_v$ under B, and $t^T_v = t^F_v$ under $B \cup \{w\}$. Hence, the shortest path from $B \cup \{w\}$ to v must begin with w, otherwise it contradicts the condition. Therefore, w contributes to the loss reduction.

The above cases concluded that $\bar{r}_X(B \cup \{w\} \rightarrow v) = \bar{r}_X(\{w\} \rightarrow v)$. Let $A \subseteq B$, similar to the situation of B, we can get $\bar{r}_X(A \cup \{w\} \rightarrow v) = \bar{r}_X(\{w\} \rightarrow v) = \bar{r}_X(B \cup \{w\} \rightarrow v)$. Besides, the monotonicity of $\bar{r}$ implies that $\bar{r}_X(A \rightarrow v) \leq \bar{r}_X(B \rightarrow v)$, therefore, $\bar{r}_X(A \cup \{w\} \rightarrow v) - \bar{r}_X(A \rightarrow v) \geq \bar{r}_X(B \cup \{w\} \rightarrow v) - \bar{r}_X(B \rightarrow v)$. Since $\bar{r}(S_T \rightarrow v)$ is the weighed aggregation of $\bar{r}_X(S_T \rightarrow v)$ and $\overline{\mathbb{R}}$ is the linear aggregation of $\bar{r}$, thus $\overline{\mathbb{R}}$ is submodular, the proof ends. □

Empirical Analysis. We compare the tightened upper bound with the ordinary one mentioned in Lemma 3 in § 7.2, the results show that the new bound can improve the approximation by about 5% on average, proving the effectivity of it.

5 FAIR-TLRM ALGORITHMS

Traditional truth maximization approaches [6] for rumor mitigation often overlook the differing loss weights among users and do not adequately address fairness concerns (§ 1). To tackle these issues, we introduce Fair-Greedy, a dual-objective optimization algorithm tailored for FAIR-TLRM problem (§ 5.1). Recognizing the high computational demands of Fair-Greedy on large networks, we propose FWS-RM (§ 5.2), a scalable alternative that utilizes a novel group-aware weighted reverse influence sampling method alongside the aforementioned sandwich approximation technique.

5.1 Greedy Baseline

Revisiting Saturate algorithm. Krause et al. [25] proposed the Saturate algorithm to identify a set that satisfies the Maxmin constraint. The core idea is to greedily select candidates that yield the largest marginal gain for all groups, i.e., "saturate", by truncating the objective function. Specifically, it establishes a fairness threshold opt', ensuring that each group's influence is bounded by this value, thereby facilitating the identification of candidates that maximize the overall influence. In our context, the key is to truncate the maximum ratio of users each group can save to opt' (where opt' is determined through bisection in $[0, 1]$ and serves as the fairness constraint). We then employ a set-cover algorithm to assess the effectiveness of opt' until the optimal solution is found.

Algorithm 1 FAIR-Greedy

Input: G, S_F, b, α
Output: S_T

1: Initialize $S_T = \emptyset$
2: Get $S_T^{'}$ and $opt^{'}$; the solution satisfies the $opt^{'}$-fairness constraint and the maximum fairness score
3: Define $f_\alpha(S_T) := \frac{1}{c}\sum_{i=1}^{c} \min\{1, \frac{\mathbb{R}_i(S_T)}{\alpha \cdot opt^{'} \cdot \mathbb{L}_i(G, C_i, S_F, \emptyset)}\}$
4: **while** $|S_T| < b$ and $f_\alpha(S_T) < 1$ **do**
5: $\quad v^* \leftarrow \arg\max_{v \in V \setminus (S_F \cup S_T)} f_\alpha(S_T \cup \{v\}) - f_\alpha(S_T)$
6: $\quad S_T \leftarrow S_T \cup \{v^*\}$
7: **if** $f_\alpha(S_T) < 1$ **then**
8: $\quad$ **Return** $S_T^{'}$
9: **while** $|S_T| < b$ **do**
10: $\quad v^* \leftarrow \arg\max_{v \in V \setminus (S_F \cup S_T)} \mathbb{R}(S_T \cup \{v\}) - \mathbb{R}(S_T)$
11: $\quad S_T \leftarrow S_T \cup \{v^*\}$
12: **Return** S_T

Fair-Greedy. Algorithm 1 presents our basic Fair-Greedy. We start by initializing an empty seed set for the truth campaign (Line 1). Next, we leverage Saturate [25] to find the truth set $S_T^{'}$ that satisfies the $opt^{'}$-fairness constraint, with the maximum fairness score $opt^{'}$ (Line 2). Using this $opt^{'}$, we define the truncated objective function $f_\alpha(S_T)$ as mentioned in Saturate (Line 3). We then iteratively choose the node v^* that maximizes the $f_\alpha(S_T)$ until the objective reaches 1 (Line 4-6). If the size of S_T has reached b, but $f_\alpha(S_T)$ does not meet the requirements yet, we return $S_T^{'}$ as the result (Line 7-8). However, if the fairness criteria are fulfilled and the size of S_T is still below b, we will continue to greedily add nodes that maximize the reward until the size of S_T equals b (Line 9-12).

5.2 Scalable Optimization via Reverse Sampling

Algorithm 1 (Fair-Greedy) requires extensive computations of mitigation rewards to identify candidates for the truth campaign that maximize the increase in $\mathbb{R}(S_T)$ while satisfying the fairness constraint. Calculating the exact influence spread $\sigma(S_T)$ under the CIC model is known to be #P-hard [64], and determining the loss reduction under the TCIC model is even more challenging due to the intricate tie-breaking policies involved.

Previous research [4, 51, 52] has focused on advanced *reverse influence sampling* (RIS) to address the influence maximization (IM) problem. In the traditional RIS approach, a node v is sampled uniformly at random from G, and a reverse BFS from v is performed to generate a RR-Set, which consists of the nodes reachable from v. The influence spread of a seed set is then estimated by its coverage across multiple RR-Sets. Recently, [18] proposed SUBSIM, an improved sampling method for generating RR-Sets more efficiently. However, these works cannot be extended to solve ours easily. First, traditional RIS starts by sampling a random node from G, whereas the TLRM problem requires sampling nodes affected by rumors. Unlike the well-known targeted IM [30] variant, we do not know in advance which users are influenced by rumors, making it challenging to initiate reverse propagation. Second, in standard RIS, a seed set's expected influence is proportional to the number of RR-Sets it covers, treating all RR-Sets equally. However, in our settings, where nodes have varying weights, applying this approach without adjustment could yield suboptimal truth seed sets. Finally, the fact that nodes belong to different groups introduces additional complexity. Traditional RR-Set indexing methods, which do not consider group structure, are unsuitable for maintaining fairness constraints. While a naive solution might involve building an index for each group, this would introduce unnecessary memory consumption and reduce efficiency. To tackle these limitations, we designed a novel RR-Set generation scheme that is effective and efficient for our *Fair-TLRM* problem.

Weighted RR-Set Generation for Grouped Nodes. Algorithm 2 presents the pseudo-code of GRASS(Group-aware Weighted RR-Sets Generation Scheme). The process starts by performing a forward propagation simulation rooted at the rumor source S_F, identifying the nodes influenced by the rumor (denoted as Inf_f), and recording the time t_F when the rumor arrives at them (Line 1), in this way we find the nodes to initiate reverse propagation. Next, a node is randomly selected from Inf_F as the start node, along with its time t_F (Line 2). Reverse Dijkstra is then applied to trace back and find nodes capable of "save" r the rumor-affected node, adding them to the RR-set. During this process, SUBSIM is used to accelerate generation (Lines 3–17). Finally, the reward w_i of this RR-set and the group c_i to which it belongs are packed into a tuple and returned (Lines 18–19). In order to obtain the optimal solution, with the returning tuple, for each user v, we record the indexes of the RR-Sets it covers, along with the reward weights. Since the w_i differs among RR-Sets, we use *Monotone Stack* as the data structure for efficient computation for weighted max-cover algorithm. Besides, through the returning tuple, we know the group of the "saved" node for each RR-Set, we then build id-group indexes for each RR-Set that are effective for latter group loss reduction calculation. For a given user set U and a random RR set R, we define a random variable $Y(U, R)$ such that $Y(U, R) = w_i$ if $U \cap R_i \neq \emptyset$, and $Y(U, R) = 0$ otherwise, where w_i is the reward of R_i. The expected influence $\mathbb{R}(S_T)$ under the TCIC model is equal to $INF \cdot \mathbb{E}[Y(U, R)]$

Algorithm 2 GRASS

Input: $G, S_F, \mathcal{W}, C$
Output: A RR-Set R, its weight w and its group gc

1: $Inf_F, t_F \leftarrow$ The set of rumor-influenced nodes and their distance from F through a forward propagation of S_F
2: $r, t_r^F \leftarrow$ A random node and its dist in Inf_F, t_F
3: $R \leftarrow \{r\}$
4: priority_queue Q = [{$r, 0$}]
5: **while** $Q \neq \emptyset$ **do**
6: $\quad$ Let $\{u, dd\}$ be the top element of queue Q and pop it;
7: $\quad$ Let u[i] (i = 1,2,...) be the i-th in-neighbor of u;
8: $\quad p = 1/d_{in}(u)$;
9: $\quad rand$ = a random number from 0 to 1 generated in uniform;
10: $\quad i = \lceil (\frac{\log(\text{rand})}{\log(1-p)}) \rceil$;
11: $\quad$ **while** $i \leq d_{in}(u)$ **do**
12: $\quad\quad v \leftarrow u[i]$
13: $\quad\quad$ **if** $v \notin R$ **and** $dd + d_{uv}^p < t_u^F$ **then**
14: $\quad\quad\quad R \leftarrow R \cup \{v\}$
15: $\quad\quad\quad Q.push(\{v, dd + d_{uv}^p\})$
16: $\quad\quad rand$ = a random number from 0 to 1 generated in uniform;
17: $\quad\quad i+ = \lceil (\frac{\log(\text{rand})}{\log(1-p)}) \rceil$;
18: $w \leftarrow \mathcal{W}$[r]
19: $gc \leftarrow C$[r]
20: **Return** R, w, gc

FWS-RM. Building on Fair-Greedy and the group-sensitive RR-Set generation method, we propose the FWS-RM algorithm (Fairness-aware Weighted-RIS-Based Solution to Rumor Mitigation). Like Fair-Greedy, FWS-RM first ensures fairness by selecting the minimum number of nodes necessary to meet the fairness constraint. It then iteratively picks nodes that maximize marginal loss reduction. As mentioned earlier, computing the exact value of $\mathbb{R}(S_T \cup v) - \mathbb{R}(S_T)$ is computationally intractable in polynomial time, so we leverage the RIS technique to approximate this value. By generating a sufficient number of RR-Sets, we can guarantee a near-optimal expected reward from S_T. As demonstrated in previous work [42], without the fairness constraint, if the number of RR-Sets exceeds a threshold N_{max}—defined by Eq.(11) with $\Delta = \frac{8}{9}\delta$—the seed set S_T is a $(1-1/e-\epsilon)$-approximate solution with probability at least $1-\delta$. In the Rumor Mitigation (RM) problem, a node v must first be reached by S_F for S_T to gain any reward. To estimate the lower bound (LB) of the loss reduction, we calculate the probability that a randomly selected node is influenced by S_F. This probability vector is computed via BFS, and the lower bound is given by $LB \geq r \cdot \sum_{v \in MAS} pro(v)$, where $pro(v)$ represents the probability that v is reached by S_F, and r is the smallest node weight in MAS.

$$N_{max} = \frac{8n(3+\epsilon^{'})(1-1/e)[ln\frac{27}{4\Delta} + ln\binom{n}{k}]}{3LB[\epsilon(1+\epsilon^{'}) - 2\epsilon^{'}(1-1/e)]^2} \tag{11}$$

Algorithm 3 provides the pseudo-code for FWS-RM. The algorithm operates within an OPIM framework, utilizing two sets of RR-Sets: $\mathcal{R}_1$ to generate the seed set S_T, and $\mathcal{R}_2$ to evaluate its effectiveness. Both the lower and upper bounds on $\mathbb{R}(S_T)$ are derived from these sets. Formally,

$$\mathbb{R}^u(S^o) = (\sqrt{\frac{\Lambda_1(S^*)}{1-1/e} + ln(1/\delta_1)} + \sqrt{ln(1/\delta_1)})^2 \frac{n}{\theta_1(1-\epsilon^{'})} \tag{12}$$

$$\mathbb{R}^l(S^*) = ((\sqrt{\Lambda_2(S^*) + \frac{25ln(1/\delta_2)}{36}} - \sqrt{ln(1/\delta_2)})^2 - \frac{ln(1/\delta_2)}{36}) \frac{n}{\theta_2(1+\epsilon^{'})} \tag{13}$$

Specifically, $\Lambda_1(S^*)$ (resp. $\Lambda_2(S^*)$) is the reward covered by S^* in $\mathcal{R}_1$ (resp. $\mathcal{R}_2$). Moreover, as demonstrated in [60], when solving the dual-objective optimization problem, the strategy that first uses local search to find partial solutions that satisfy the constraints, then uses a greedy approach to maximize the submodular objective function under the RIS framework, a $(1-1/e-\epsilon)$-approximation can be obtained with at least $(1-\delta)$ probability.

Time Complexity of FWS-RM. Since the main time cost of the FWS-RM comes from the generation of RR-Sets, the time complexity of FWS-RM is $O(\sum_{R \in \mathcal{R}_1 \cup \mathcal{R}_2}(INF_F + \frac{m}{n} \cdot (INF_1)^2)$, where INF_F is the expected influence spread of S_F and INF_1 is the largest reverse expected influence spread of the node r in G.[9]

Sandwich Algorithm. Drawing upon the previously discussed findings, we incorporate the sandwich method in Algorithm 4. This yields the optimal seed set $S_T^* \in \{S_T^L, S_T^U\}$, which results in the maximum objective value with respect to our original goal.

[9]Proof can be found in the appendix.

Algorithm 3 FWS-RM

Input: G, S_F, b, α, ϵ, δ
Output: S_T

Initialize $S_T = \emptyset$
$\delta^{'} \leftarrow \frac{\delta}{9}$, $\epsilon^{'} \leftarrow \frac{\epsilon}{2}$, $\Delta \leftarrow \frac{8\delta}{9}$
Set N_{max} according Eq.(11), $N_0 = N_{max} \cdot \epsilon^2 \frac{LB \cdot ln(1/\delta)}{4n}$
Compute $INF_F^{'}$; an $(\epsilon^{'}, \delta^{'})$-approximation of INF_F
Generate two sets $\mathcal{R}_1$ and $\mathcal{R}_2$ of random RR-sets by algorithm 2, with $|\mathcal{R}_1| = |\mathcal{R}_2| = \theta_0$
$i_{max} \leftarrow \lceil \frac{N_{max}}{N_0} \rceil$
for $i \leftarrow 1$ **to** i_{max} **do**
    $S_T^* \leftarrow$ WeightedMaxCover($\mathcal{R}_1$,b,n)
    Compute $\mathbb{R}^l(S_T^*)$ and $\mathbb{R}^u(S_T^o)$ according to (13) and (12), where $\delta_1 = \delta_2 = \Delta/(3i_{max})$
    $z \leftarrow \mathbb{R}^l(S_T^*)/\mathbb{R}^u(S_T^o)$
    if $z \geq (1-1/e-\epsilon)$ **or** $i = i_{max}$ **then**
        Break
    Double the size of $\mathcal{R}_1$ and $\mathcal{R}_2$ with new RR-Sets
Get $S_T^{'}$ and opt; the solution satisfies the $opt^{'}$-fairness constraint and the maximum fairness score
Define $f_\alpha(S_T) := \frac{1}{c}\sum_{i=1}^{c} \min\{1, \frac{INF_F^{'} \cdot \mathbb{E}_i[Y(S_T,R)]}{\alpha \cdot opt^{'} \cdot \mathbb{L}_i(G,C_i,S_F,\emptyset)}\}$
while $|S_T| < b$ and $f_\alpha(S_T) < 1$ **do**
    $v^* \leftarrow \arg\max_{v \in V \setminus (S_F \cup S_T)} f_\alpha(S_T \cup \{v\}) - f_\alpha(S_T)$
    $S_T \leftarrow S_T \cup \{v^*\}$
if $f_\alpha(S_T) < 1$ **then**
    Return $S_T^{'}$
if $|S_T| < b$ **then**
    for $i \leftarrow 1$ **to** b **do**
        if i-th item of S_T^* **Not** in S_T **then**
            $v^* \leftarrow i$-th item of S_T^*
            $S_T \leftarrow S_T \cup \{v^*\}$
        if $|S_T| = b$ **then**
            Break
Return S_T

Algorithm 4 Sandwich Algorithm

Input: G, S_F, b, $\underline{\mathbb{R}}$, $\overline{\mathbb{R}}$
Output: S_T^*

$S_T^U \leftarrow$ FWS-RM($G, S_F, b, \overline{\mathbb{R}}$)
$S_T^L \leftarrow$ FWS-RM($G, S_F, b, \mathbb{R}$)
$S_T^* = \arg\max_{S_T \in \{S_T^U, S_T^L\}} \mathbb{R}(S_T)$
Return S_T^*

6 TRADE-OFF: FAIRNESS AND REWARD

In this section, we present several insightful case studies as a complementary contribution. Our algorithm aids online social network owners in minimizing losses through truth campaigns while ensuring fairness. However, our experimental explorations reveal that the performance of FWS-RM varies significantly across different networks, particularly when networks are partitioned into distinct groups based on attributes such as age or gender. For instance, in niche groups with weak internal connections, applying FWS-RM may not yield the desired outputs. To illustrate this, we applied algorithm 3 on a real-world social network *LastFM*[10], a social network established via public API in March 2020. This dataset categorizes users into 18 groups primarily based on location information. We

[10]https://snap.stanford.edu/data/feather-lastfm-social.html

randomly selected *20* nodes as fake seeds for our experiment, setting the fairness parameter α to *0.9*. Subsequently, we launched a truth campaign of size *20*.

Figure 6: The structure of relations in group 4

In group 4 of the *LastFM* dataset, nodes exhibit very limited internal connections, as illustrated in Figure 6. While there are some external connections from group 4 nodes to other groups, a seed from group 4 struggles to impact users within its own group directly. Conversely, seeds from other groups can only reach a small portion of users in group 4, rendering fairness considerations impractical in this scenario. When comparing the performance of FWS-RM with the fairness-agnostic algorithm WSRM, we found that the loss reduction achieved by FWS-RM amounted to only **60.17%** of the reward obtained from WSRM. This observation prompts us to identify several factors that hinder the effectiveness of the fairness constraint in practical applications, thereby assisting algorithm users in making informed decisions about its implementation.

6.1 Empirical Studies and Suggestions

We conducted several case studies across different real-world social networks and presented the results about two identified key factors: **(i)** the impact of the truth set budget on the algorithm's reward, **(ii)** the effect of the relative propagation speeds of rumor and truth. These help characterize the better-performing social networks for more effectively mitigating losses caused by rumors while maintaining fairness constraints. Although our tests were conducted on all our datasets (§ 7), we only present the results on two representative ones, Facebook (connections are dense) and LastFM (featuring dispersed connections).

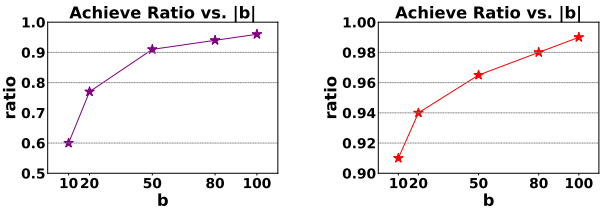

(a) LastFM (b) Facebook

Figure 7: Achieve ratio vs. $|b|$

Impact of Budget Size. Figure 7 shows that as b increases, the achieved ratio (the ratio of the reward obtained by applying FWS-RM to that of WSRM) improves across both datasets, simply because a larger budget gives the algorithm more flexibility to balance the trade-off between loss reduction and fairness. Additionally, nodes contributing to fairness can create the "combination effect" (see Section 3), enhancing overall performance when b is larger. Notably, in the *LastFM* dataset, the achieved ratio remains low when b is small—a scenario common in practice due to financial constraints limiting the size of the seed set. However, the *Facebook* dataset does not observe this effect. This difference likely stems from the structural characteristics of the networks. In practice, for datasets with sparse connections like *LastFM*, *allocating less than 0.5% of the total users as seed nodes can lead to a significant negative impact on loss reduction when fairness is factored in.*

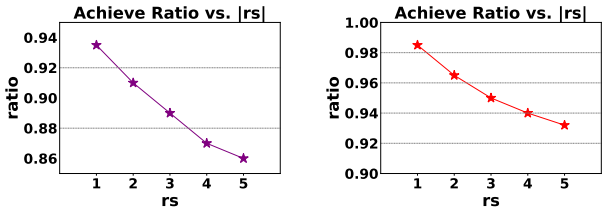

(a) LastFM (b) Facebook

Figure 8: Achieve ratio vs. $|rs|$

Impact of the Relative Propagation Speed of Rumor and Truth. In practical applications, slowing down the spread of rumors, such as by muting certain users, can alter the relative spread speed of rumor and truth. As shown in Figure 8, where the rs represents the relative speed ratio (i.e., $\mathbb{E}[d_e^T / d_e^F]$), our empirical study reveals that as the relative speed of rumors decreases, the achieve ratio increase. This suggests that when rumors spread more slowly, truth campaigns can intervene more effectively, allowing for a better balance between minimizing losses and maintaining fairness. *Thus, identifying the rumor source quickly and imposing the in-time interventions can improve the performance of fairness-aware algorithms in real-world applications.*

Characteristics of Better-performing Social Networks. We analyzed node characteristics in both the *LastFM* and *Facebook* datasets. Specifically, we calculated various metrics, including harmonic centrality [34] (which reflects connectivity between nodes), out-degree, in-degree, node weight, and rumor reach probability (the likelihood that a path exists from S_F to v). The results represent the average values within each group. Specifically, for the other four metrics, there is no obvious difference between the group with a large impact on reward and the group with a small impact.Our observations reveal that harmonic centrality has the greatest influence on fairness—groups with higher harmonic centrality tend to exhibit better fairness performance. This indicates that *tightly connected nodes within a group can more easily propagate truth, allowing fairness to be achieved with minimal sacrifice in reward.* Table 4 presents the harmonic centrality of the group that most impacts the reward in both LastFM and Facebook. HCW means harmonic centrality of the nodes within the group while HCIE means harmonic centrality between the internal nodes and external nodes. In LastFM, the worst-performing group had no internal connections and very few external links, which significantly lowered the reward when fairness constraints were applied, especially when b was small. In contrast, Facebook did not exhibit this issue.

Table 4: Harmonic Centrality of the group that has the greatest impact on loss reduction in LastFM and Facebook.

Metric \ Datasets	LastFM	Facebook
HCW	0	0.145
HCIE	0.156	0.166

Joint-Greedy framework. Building on the insights from the experiments, we introduce a *Joint-Greedy Framework* tailored for

datasets like *LastFM*. This framework uses a reward-fairness balance factor, p, to determine whether to apply FWS-RM or WSRM. In the Joint-Greedy framework, a random number r is uniformly sampled from the interval $[0, 1]$. If $p \geq r$, the framework selects FWS-RM, detailed in Algorithm 3. Otherwise, it opts for WSRM, a simplified version of FWS-RM that focuses solely on minimizing the platform's economic losses by mitigating rumor spread without considering fairness constraints. This approach balances the trade-off between reward and fairness by adapting based on the value of p. It is straightforward to show that the Joint-Greedy framework, with a probability distribution over policies, can improve the expected value of the reward. The full details of the Joint-Greedy framework are provided in Algorithm 5.

Algorithm 5 JOINT-Greedy

Input: $G, S_F, b, \alpha, p, \epsilon, \delta$
Output: S_T
1: $r \leftarrow rand(0, 1)$
2: **if** $p \geq r$ **then**
3: $S_T \leftarrow$ FWS-RM$(G, S_F, b, \alpha, \epsilon, \delta)$
4: **else**
5: $S_T \leftarrow$ WSRM$(G, S_F, b, \epsilon, \delta)$
6: **Return** S_T

7 EXPERIMENTS

We empirically evaluate our proposed algorithms in this section. All methods are implemented in C++ and executed on a server with Intel(R) Xeon(R) 2.20 GHz CPU and 128GB of RAM.

7.1 Experimental Settings

Datasets. We evaluate our algorithms with five real-world datasets, namely, EmailCore [29], Twitch [29], Facebook [35], Digg [28], and Weibo [63]. Table 5 shows the details of each dataset. Specifically, Facebook is grouped by age, Twitch is grouped by country, Weibo is grouped by gender and the grouping situation of EmailCore comes with the dataset itself. Since Digg does not contain attributes for grouping, we complemented it by synthetically generated user attributes which overall fit is publicly-known distributions in Digg. Following [50–52], for each dataset, we use the *weighted-cascade model* [24] to determine the edge-weight, i.e., $p_{u,v} = 1/|N_{in}(v)|$, where $|N_{in}(v)|$ is the number of v's in-neighbors.

Algorithms. We compare a set of algorithms in experiments.

- **FWS-RM**: Our proposed algorithm which considers both individual losses and the fairness constraint.
- **WSRM**: a simplified version of FWS-RM without considering fairness issue and solely minimizes the losses.
- **EIL-Greedy**[6]: a method that only maximizes the number of user *successfully rescued* by truth, without considering individual losses and fairness constraint.
- **Fair-MC**: a lazy-forward technical-equipped MC-Based method extended from CELF++ [17], considering both individual losses and fairness constraints.
- **Weighted out-neighbors**: a method selects top-k nodes with the largest weights from S_F's out-neighbors as the truth set.

Default Parameters. We evaluate the performance of algorithms on different parameters, including the budget b, the fairness threshold α, and the sampling error factor ϵ. We set the default $b = 50$ for *EmailCore* and *Facebook*, $b = 100$ for *Digg*, *Twitch* and *Weibo*, and $\alpha = 0.8$ for all datasets. Following [1, 19], we set $\epsilon = 0.2$ for small datasets like *EmailCore* and *Facebook*,and $\epsilon = 0.3$ for *Digg*, *Twitch* and *Weibo* as the default values. We estimate the loss reduction by using $2^4 \times 10^5$ *RR-Sets* [19, 21], generated independently of the considered algorithms. We terminate an algorithm if it cannot finish in 48 hours and use OOT (i.e., out of time) to represent the result.

Table 5: Dataset Statistics

Dataset	$n = \|V\|$	$m = \|E\|$	d_{avg}	$c = \|C\|$	Type
EmailCore	1,005	25,571	25.4	42	Directed
Facebook	1,216	42,443	69.8	4	Undirected
Digg	68,634	1,242,541	18.1	6	Directed
Twitch	168,114	6,797,557	5.3	21	Undirected
Weibo	1,787,443	83,135,996	46.5	2	Directed

Evaluation Metrics. We employ the losses reduction, running time and fairness score (FS) as evaluation metrics in experiments. Specifically, the losses reduction is the decrease in loss after we launch the truth set. The fairness score is used to measure the fairness of the algorithms, as computed in the following equation:

$$FS = \min_{C_i \in C} \frac{\mathbb{L}_i(G, C_i, S_F, \emptyset) - \mathbb{L}_i(G, C_i, S_F, S_T)}{\mathbb{L}_i(G, C_i, S_F, \emptyset) \cdot opt}$$

Following [42], we use 20K Monte Carlo to simulate the loss reduction of final solution. We run each method three times and report the average results.

7.2 Evaluation of FWS-RM Algorithm

In this set of experiments, we evaluate the performance of FWS-RM algorithm. Note that, due to space limitations, we only show the experimental results that use network topology to calculate the individual losses. The full experiment results can be found in [14].

Varying the Budget b. We study the effect of budget b on the loss reduction, running time, and fairness score. We vary b from 10 to 100 for small datasets, and 20 to 200 for large datasets. As shown in Figure 9-11, when b grows, the loss reductions across five algorithms increase, the reason is that as b increases, the number of spreaders disseminating the truth grows, leading to a corresponding increase in loss reduction. Moreover, the FWS-RM, WSRM and Fair-MC significantly outperform EIL and Weighted-ON in terms of loss reduction. We can observe that it becomes apparent that the loss reduction yielded from FWS-RM and WSRM exhibit negligible differences in the Digg, Weibo and Facebook datasets, with the former achieving a staggering 95% approximation of the WSRM' reduction value. In the remaining two datasets, when b is small, WSRM performs relatively better compared with FWS-RM. The reason can be found in Section 6. It is worth mentioning that FWS-RM significantly improves fairness, and a runtime analysis reveals that satisfying fairness does not incur a significant time overhead, typically only about 1% of the total runtime.

Varying the error factor ϵ. We study the impact of error factor on loss reduction, running time and fairness score by varying ϵ from 0.1 to 0.3. Since only FWS-RM, WSRM and EIL provide a theoretical guarantee, we show the result of these three algorithms. In Figure 13-15, it can be observed that as ϵ increases, the reduction loss decreases slightly, this is because when ϵ is small, the number of RR-Sets is of great largeness, the difference between the upper

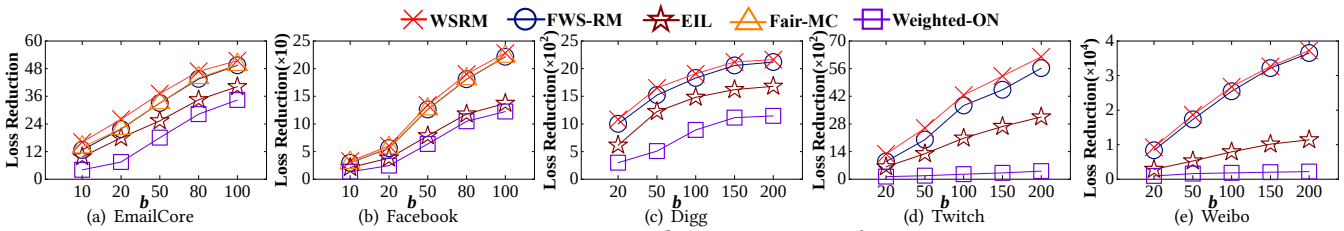

Figure 9: Reduction Losses vs. b

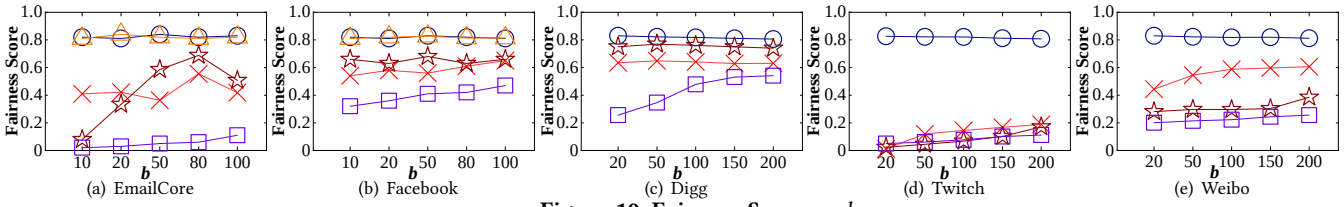

Figure 10: Fairness Score vs. b

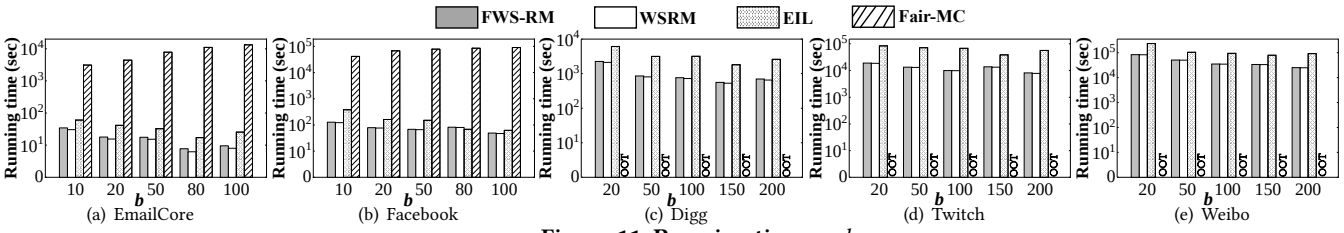

Figure 11: Running time vs. b

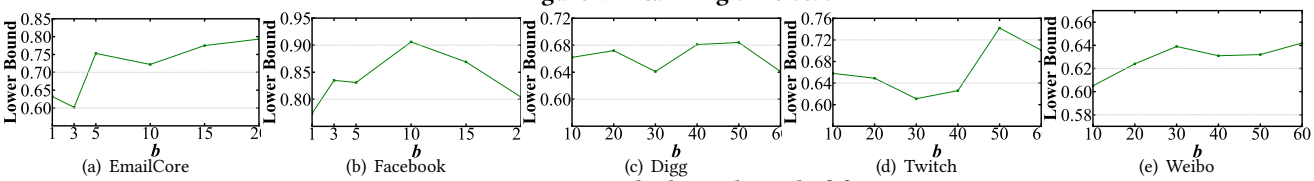

Figure 12: The lower bound of β

and lower bounds is smaller, that is, the bounds are tighter and the results are closer to actual reward that with more loss reduction, thus the calculated value is larger. Meanwhile, as ϵ increases, the running times of the three algorithms decreases and their respective fairness scores increase, the reason is that as ϵ increases, the error of the algorithm increases, and the denominator decreases accordingly when calculating FS, causing FS to rise slightly. Another observation is that TLRM problems often require shorter running times than RM problems. Although they both use the OPIM framework, TLRM tends to meet the accuracy requirements in fewer rounds, which allows it to generate fewer RR-Sets and reduce the time cost, that is why FWS-RM and WSRM usually run faster than EIL.

Varying the α. We evaluate the impact of α (i.e., the threshold we use to satisfy the fairness constraint) on loss reduction and running time. Since only FWS-RM uses the fairness parameter α, we compare the loss reduction (i.e., effectiveness) and running time (i.e., efficiency) of FWS-RM by varying α from 0.1 to 0.9 and the result is displayed in Figure 16. We can observe that as α increases, loss reduction decreases within the range of 5%-9%, which suggests that FWS-RM enhance the fairness of the algorithm at the cost of a slight reward reduction. Moreover, as α increases, the running time rises slightly. This is due to the additional time required by the algorithm to meet the stricter fairness constraints.

Lower Bound. Figure 12 shows the lower bounds of β. It is easy to find that among all datasets $\beta > 0.6$, proving the tightness of our bound. Besides, we also compared our lower bound with the bound mentioned in Lemma 3. Our tightness improved by about 5% on average, proving that our new bound is tighter[11].

7.3 Additional Tests

In this part, we conduct experiments on calculating the number of overlaps in the truth seed sets selected by TLRM and RM (which only minimizes the number of people affected by the rumor) to further illustrate the difference between the two problems.

In the experiment, we set the number of rumor seed nodes as **50**. In order to mitigate the effects of stochasticity, we conduct three separate tests in all node-weight set methods. Notably, for random node-weight set function, the individual losses of each user are randomized and selected from the set $\{0.1, 0.5, 0.8\}$. The average value derived from these tests served as the final experimental outcome. The table delineates the extent of overlap between truth sets chosen by TLRM and RM. Note that once the budget surpasses 300, the increase in loss reduction of the truth set becomes negligible and the truth set parallels the one where the budget is 300. Hence, results beyond this point have not been included for consideration.

Table 6 shows insights garnered from the experimental findings. It can be seen that, when varying budgets and individual loss set methods, the overlap ratio between the truth sets selected by TLRM and RM among three datasets ranges from 30% to 40% and averages

[11]The detailed result is in the appendix.

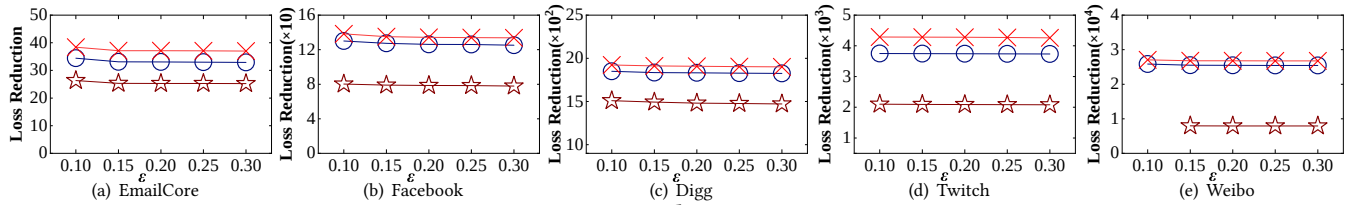

(a) EmailCore (b) Facebook (c) Digg (d) Twitch (e) Weibo

Figure 13: Reduction Losses vs. ϵ

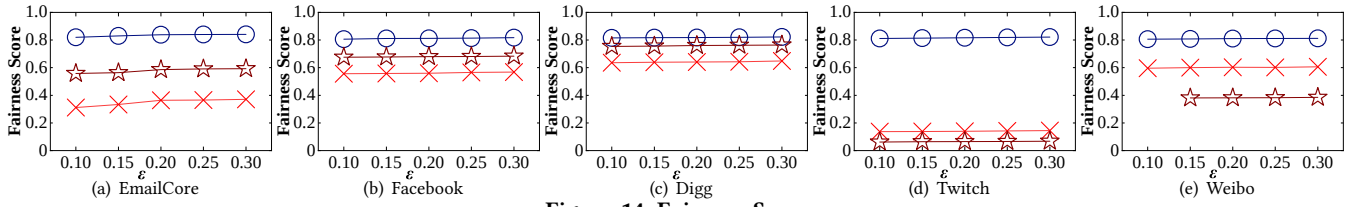

(a) EmailCore (b) Facebook (c) Digg (d) Twitch (e) Weibo

Figure 14: Fairness Score vs. ϵ

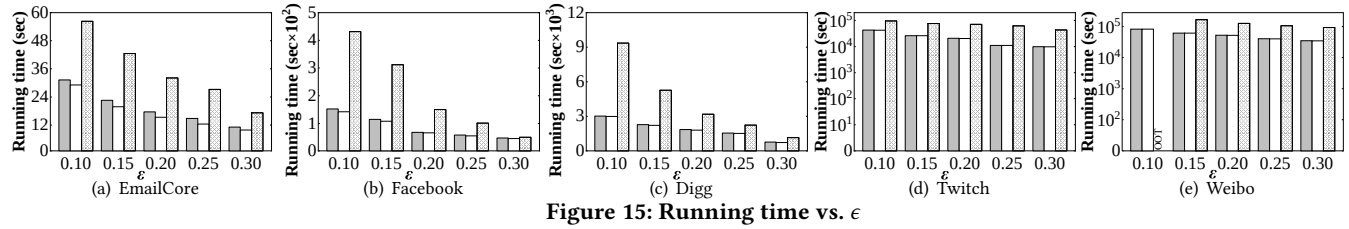

(a) EmailCore (b) Facebook (c) Digg (d) Twitch (e) Weibo

Figure 15: Running time vs. ϵ

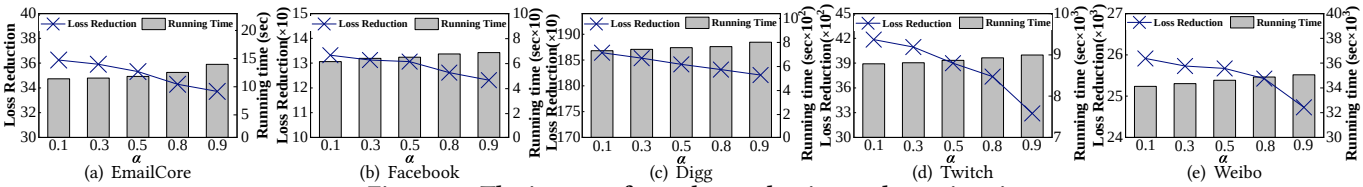

(a) EmailCore (b) Facebook (c) Digg (d) Twitch (e) Weibo

Figure 16: The impact of α on loss reduction and running time

around 1/3, suggesting that the overlap rate of the truth sets consistently maintains at a low frequency. This emphasizes that our problem is significantly different from existing RM problems.

Table 6: The overlaps of S_T between TLRM and RM

Node-weight set way	Topology			Historical			Random		
Datasets / $\|b\|$	Digg	Twitch	Weibo	Digg	Twitch	Weibo	Digg	Twitch	Weibo
50	20	16	22	19	20	22	18	12	21
100	44	38	43	40	36	41	38	37	42
200	56	49	63	50	47	53	48	43	54
300	100	89	111	105	98	109	87	82	91

8 CONCLUSION

In this work, we study a novel problem Fair-TLRM that aims to minimize the losses caused by rumor while considering user engagement and fairness together. We develop a dual-objective optimization algorithm Fair-Greedy, propose its scalable version FWS-RM with data-dependent approximation guarantee by employing a novel group-aware weighted-RIS and sandwich technical. Additionally, we study the impact of fairness on algorithm behaviours through several case studies, drawing a series of fruitful conclusions and proposing a framework called Joint-Greedy for better algorithm-performing. Experiments over five real-world datasets demonstrate the effectiveness and efficiency of our algorithm.

REFERENCES

[1] Cigdem Aslay, Francesco Bonchi Laks VS Lakshmanan, and Wei Lu. 2017. Revenue Maximization in Incentivized Social Advertising. *Proceedings of the VLDB Endowment* 10, 11 (2017).

[2] Shishir Bharathi, David Kempe, and Mahyar Salek. 2007. Competitive influence maximization in social networks. In *Internet and Network Economics: Third International Workshop, WINE 2007, San Diego, CA, USA, December 12-14, 2007. Proceedings 3*. Springer, 306–311.

[3] Phillip Bonacich and Paulette Lloyd. 2001. Eigenvector-like measures of centrality for asymmetric relations. *Social networks* 23, 3 (2001), 191–201.

[4] Christian Borgs, Michael Brautbar, Jennifer Chayes, and Brendan Lucier. 2014. Maximizing social influence in nearly optimal time. In *Proceedings of the twenty-fifth annual ACM-SIAM symposium on Discrete algorithms*. SIAM, 946–957.

[5] Sergey Brin and Lawrence Page. 1998. The anatomy of a large-scale hypertextual web search engine. *Computer networks and ISDN systems* 30, 1-7 (1998), 107–117.

[6] Ceren Budak, Divyakant Agrawal, and Amr El Abbadi. 2011. Limiting the spread of misinformation in social networks. In *Proceedings of the 20th international conference on World wide web*. 665–674.

[7] Taotao Cai, Jianxin Li, Ajmal Mian, Rong-Hua Li, Timos Sellis, and Jeffrey Xu Yu. 2020. Target-aware holistic influence maximization in spatial social networks. *IEEE Transactions on Knowledge and Data Engineering* 34, 4 (2020), 1993–2007.

[8] Wei Chen, Yifei Yuan, and Li Zhang. 2010. Scalable influence maximization in social networks under the linear threshold model. In *2010 IEEE International Conference on Data Mining (ICDM)*. 88–97.

[9] Peng Cheng, Xiang Lian, Lei Chen, and Siyuan Liu. 2020. Maximizing the utility in location-based mobile advertising. *IEEE Transactions on Knowledge and Data Engineering* 34, 2 (2020), 776–788.

[10] Xuejun Ding, Xiaxia Zhang, Ruoshi Fan, Qiaochu Xu, Kyle Hunt, and Jun Zhuang. 2022. Rumor recognition behavior of social media users in emergencies. *Journal of Management Science and Engineering* 7, 1 (2022), 36–47.

[11] Pedro Domingos and Matt Richardson. 2001. Mining the network value of customers. In *Proceedings of the seventh ACM SIGKDD international conference on Knowledge discovery and data mining*. 57–66.

[12] Lidan Fan, Zaixin Lu, Weili Wu, Bhavani Thuraisingham, Huan Ma, and Yuanjun Bi. 2013. Least cost rumor blocking in social networks. In *2013 IEEE 33rd International Conference on Distributed Computing Systems*. IEEE, 540–549.

[13] Golnoosh Farnad, Behrouz Babaki, and Michel Gendreau. 2020. A unifying framework for fairness-aware influence maximization. In *Companion Proceedings of the Web Conference 2020*. 714–722.

[14] Jiajie Fu, Xiangyu Ke, Xueqin Chang, Yunjun Gao, and Lu Chen. 2024. Balancing: Minimizing the losses caused by rumor, considering user engagement and fairness together. https://github.com/FuJiaJie123/TLRM

[15] Satoru Fujishige. 2005. *Submodular functions and optimization*. Elsevier.

[16] Maksym Gabielkov, Arthi Ramachandran, Augustin Chaintreau, and Arnaud Legout. 2016. Social clicks: What and who gets read on Twitter?. In *Proceedings of the 2016 ACM SIGMETRICS international conference on measurement and modeling of computer science*. 179–192.

[17] Amit Goyal, Wei Lu, and Laks VS Lakshmanan. 2011. Celf++ optimizing the greedy algorithm for influence maximization in social networks. In *Proceedings of the 20th international conference companion on World wide web*. 47–48.

[18] Qintian Guo, Sibo Wang, Zhewei Wei, Wenqing Lin, and Jing Tang. 2022. Influence Maximization Revisited: Efficient Sampling with Bound Tightened. *ACM Transactions on Database Systems (TODS)* (2022).

[19] Kai Han, Benwei Wu, Jing Tang, Shuang Cui, Cigdem Aslay, and Laks VS Lakshmanan. 2021. Efficient and effective algorithms for revenue maximization in social advertising. In *Proceedings of the 2021 ACM SIGMOD International Conference on Management of Data*. 671–684.

[20] Keke Huang, Sibo Wang, Glenn Bevilacqua, Xiaokui Xiao, and Laks VS Lakshmanan. 2017. Revisiting the stop-and-stare algorithms for influence maximization. *Proceedings of the VLDB Endowment* 10, 9 (2017), 913–924.

[21] Tianyuan Jin, Yu Yang, Renchi Yang, Jieming Shi, Keke Huang, and Xiaokui Xiao. 2021. Unconstrained submodular maximization with modular costs: Tight approximation and application to profit maximization. *Proceedings of the VLDB Endowment* 14, 10 (2021), 1756–1768.

[22] Fariba Karimi, Mathieu Génois, Claudia Wagner, Philipp Singer, and Markus Strohmaier. 2018. Homophily influences ranking of minorities in social networks. *Scientific reports* 8, 1 (2018), 11077.

[23] Xiangyu Ke, Arijit Khan, and Gao Cong. 2018. Finding seeds and relevant tags jointly: For targeted influence maximization in social networks. In *Proceedings of the 2018 international conference on management of data*. 1097–1111.

[24] David Kempe, Jon Kleinberg, and Éva Tardos. 2003. Maximizing the spread of influence through a social network. In *Proceedings of the ninth ACM SIGKDD international conference on Knowledge discovery and data mining*. 137–146.

[25] Andreas Krause, H Brendan McMahan, Carlos Guestrin, and Anupam Gupta. 2008. Robust Submodular Observation Selection. *Journal of Machine Learning Research* 9, 12 (2008).

[26] Eun Lee, Fariba Karimi, Claudia Wagner, Hang-Hyun Jo, Markus Strohmaier, and Mirta Galesic. 2019. Homophily and minority-group size explain perception biases in social networks. *Nature human behaviour* 3, 10 (2019), 1078–1087.

[27] Sihyung Lee, Kyriaki Levanti, and Hyong S Kim. 2014. Network monitoring: Present and future. *Computer Networks* 65 (2014), 84–98.

[28] Kristina Lerman, Rumi Ghosh, and Tawan Surachawala. 2012. Social contagion: An empirical study of information spread on digg and twitter follower graphs. *arXiv preprint arXiv:1202.3162* (2012).

[29] Jure Leskovec and Andrej Krevl. 2014. SNAP Datasets: Stanford large network dataset collection. http://snap.stanford.edu/data.

[30] Yuchen Li, Dongxiang Zhang, and Kian-Lee Tan. 2015. Real-time targeted influence maximization for online advertisements. (2015).

[31] Wei Lu, Wei Chen, and Laks VS Lakshmanan. 2015. From competition to complementarity: comparative influence diffusion and maximization. *Proceedings of the VLDB Endowment* 9, 2 (2015), 60–71.

[32] Sarah T Malamut, Molly Dawes, and Hongling Xie. 2018. Characteristics of rumors and rumor victims in early adolescence: Rumor content and social impact. *Social Development* 27, 3 (2018), 601–618.

[33] Mohammad Ali Manouchehri, Mohammad Sadegh Helfroush, and Habibollah Danyali. 2021. Temporal rumor blocking in online social networks: A sampling-based approach. *IEEE Transactions on Systems, Man, and Cybernetics: Systems* 52, 7 (2021), 4578–4588.

[34] Massimo Marchiori and Vito Latora. 2000. Harmony in the small-world. *Physica A: Statistical Mechanics and its Applications* 285, 3-4 (2000), 539–546.

[35] Alan Mislove, Bimal Viswanath, Krishna P Gummadi, and Peter Druschel. 2010. You are who you know: inferring user profiles in online social networks. In *Proceedings of the third ACM international conference on Web search and data mining*. 251–260.

[36] Hung T Nguyen, Alberto Cano, Tam Vu, and Thang N Dinh. 2019. Blocking self-avoiding walks stops cyber-epidemics: a scalable gpu-based approach. *IEEE Transactions on Knowledge and Data Engineering* 32, 7 (2019), 1263–1275.

[37] Liqiang Nie, Xuemeng Song, and Tat-Seng Chua. 2016. *Learning from Multiple Social Networks*. Morgan & Claypool Publishers.

[38] Canh V Pham, Quat V Phu, and Huan X Hoang. 2018. Targeted misinformation blocking on online social networks. In *Asian Conference on Intelligent Information and Database Systems*. Springer, 107–116.

[39] John Rawls. 1971. Atheory of justice. *Cambridge (Mass.)* (1971).

[40] Gerard Salton and Christopher Buckley. 1988. Term-weighting approaches in automatic text retrieval. *Information processing & management* 24, 5 (1988), 513–523.

[41] Kemp Simon. 2021. Digital trends 2020: Every single stat you need to know about the internet. *TNW: Blog Podium: Post Marc* 4 (2021), 2021.

[42] Michael Simpson, Farnoosh Hashemi, and Laks VS Lakshmanan. 2022. Misinformation mitigation under differential propagation rates and temporal penalties. *Proceedings of the VLDB Endowment* 15, 10 (2022), 2216–2229.

[43] Michael Simpson, Venkatesh Srinivasan, and Alex Thomo. 2018. Reverse prevention sampling for misinformation mitigation in social networks. *arXiv preprint arXiv:1807.01162* (2018).

[44] Chonggang Song, Wynne Hsu, and Mong Li Lee. 2016. Targeted influence maximization in social networks. In *Proceedings of the 25th ACM International on Conference on Information and Knowledge Management*. 1683–1692.

[45] Chonggang Song, Wynne Hsu, and Mong Li Lee. 2017. Temporal influence blocking: Minimizing the effect of misinformation in social networks. In *2017 IEEE 33rd international conference on data engineering (ICDE)*. 847–858.

[46] Changfeng Sun, Han Liu, Meng Liu, Zhaochun Ren, Tian Gan, and Liqiang Nie. 2020. LARA: Attribute-to-feature adversarial learning for new-item recommendation. In *Proceedings of the 13th international conference on web search and data mining*. 582–590.

[47] Lichao Sun, Xiaobin Rui, and Wei Chen. 2023. Scalable Adversarial Attack Algorithms on Influence Maximization. In *Proceedings of the Sixteenth ACM International Conference on Web Search and Data Mining*. 760–768.

[48] Andrea Tagarelli and Roberto Interdonato. 2013. " Who's out there?" identifying and ranking lurkers in social networks. In *Proceedings of the 2013 IEEE/ACM international conference on advances in social networks analysis and mining*. 215–222.

[49] Andrea Tagarelli and Roberto Interdonato. 2014. Lurking in social networks: topology-based analysis and ranking methods. *Social Network Analysis and Mining* 4 (2014), 1–27.

[50] Jing Tang, Xueyan Tang, Xiaokui Xiao, and Junsong Yuan. 2018. Online processing algorithms for influence maximization. In *Proceedings of the 2018 International Conference on Management of Data*. 991–1005.

[51] Youze Tang, Yanchen Shi, and Xiaokui Xiao. 2015. Influence maximization in near-linear time: A martingale approach. In *Proceedings of the 2015 ACM SIGMOD International Conference on Management of Data*. 1539–1554.

[52] Youze Tang, Xiaokui Xiao, and Yanchen Shi. 2014. Influence maximization: Near-optimal time complexity meets practical efficiency. In *Proceedings of the 2014 ACM SIGMOD International Conference on Management of Data*. 75–86.

[53] Guangmo Tong, Weili Wu, Ling Guo, Deying Li, Cong Liu, Bin Liu, and Ding-Zhu Du. 2017. An efficient randomized algorithm for rumor blocking in online social networks. *IEEE Transactions on Network Science and Engineering* 7, 2 (2017), 845–854.

[54] Yamil R Velez, Ethan Porter, and Thomas J Wood. 2023. Latino-targeted misinformation and the power of factual corrections. *The Journal of Politics* 85, 2 (2023), 789–794.

[55] Srikar Velichety and Utkarsh Shrivastava. 2022. Quantifying the impacts of online fake news on the equity value of social media platforms–Evidence from Twitter. *International Journal of Information Management* 64 (2022), 102474.

[56] Hilde AM Voorveld, Guda Van Noort, Daniël G Muntinga, and Fred Bronner. 2018. Engagement with social media and social media advertising: The differentiating role of platform type. *Journal of advertising* 47, 1 (2018), 38–54.

[57] Soroush Vosoughi, Deb Roy, and Sinan Aral. 2018. The spread of true and false news online. *science* 359, 6380 (2018), 1146–1151.

[58] Biao Wang, Ge Chen, Luoyi Fu, Li Song, and Xinbing Wang. 2017. Drimux: Dynamic rumor influence minimization with user experience in social networks. *IEEE Transactions on Knowledge and Data Engineering* 29, 10 (2017), 2168–2181.

[59] Sheng Wen, Jiaojiao Jiang, Yang Xiang, Shui Yu, Wanlei Zhou, and Weijia Jia. 2014. To shut them up or to clarify: Restraining the spread of rumors in online social networks. *IEEE Transactions on Parallel and Distributed Systems* 25, 12 (2014), 3306–3316.

[60] Fangsong Xiang, Jinghao Wang, Yanping Wu, Xiaoyang Wang, Chen Chen, and Ying Zhang. 2024. Rumor blocking with pertinence set in large graphs. *World Wide Web* 27, 1 (2024), 1–26.

[61] Jiadong Xie, Fan Zhang, Kai Wang, Xuemin Lin, and Wenjie Zhang. 2023. Minimizing the influence of misinformation via vertex blocking. In *2023 IEEE 39th International Conference on Data Engineering (ICDE)*. IEEE, 789–801.

[62] Mao Ye, Xingjie Liu, and Wang-Chien Lee. 2012. Exploring social influence for recommendation: a generative model approach. In *Proceedings of the 35th international ACM SIGIR conference on Research and development in information retrieval*. 671–680.

[63] Jing Zhang, Biao Liu, Jie Tang, Ting Chen, and Juanzi Li. 2013. Social influence locality for modeling retweeting behaviors. In *Twenty-third international joint conference on artificial intelligence*. Citeseer.

[64] Yuqing Zhu, Deying Li, and Zhao Zhang. 2016. Minimum cost seed set for competitive social influence. In *IEEE INFOCOM 2016-The 35th Annual IEEE International Conference on Computer Communications*. IEEE, 1–9.

APPENDIX

A FULL EXPERIMENT RESULTS

This section shows the complete experiment results that are omitted in Section 7 due to space constraints (experiment results that use random and historical-activity-based individual loss weight). Specifically, in the random weight set function, we randomly selected a value from the set $\{0.1, 0.5, 0.8\}$ as the user's loss weight for three times and averaged the results. It is worth noting that EmailCore and Facebook datasets do not contain any user historical activity information, therefore, for the historical weight set way, we only conducted experiments on the Digg, Twitch, and Weibo datasets and report their results.

Varying the Budget b. The correlation between budget and factors like loss reduction, running time, and fairness score are explored through the manipulation of b. As manifested in Figure 17, 20-22, 29-31, an escalating trend in loss reduction across the five algorithms is concurrent with the upswing of b. The algorithms of FWS-RM, WSRM and Fair-MC notably outperform the other two methods in terms of loss reduction. Upon scrutinizing the results, it becomes apparent that the loss reduction yielded from FWS-RM and WSRM exhibit negligible differences in the context of the Digg, Weibo, and Facebook datasets, with the former achieving a staggering 95% approximation of the WSRM rewards. In the remaining two datasets, when b is small, FWS-RM performs relatively ordinary comparing with WSRM. The underlying reason can be found in Section 6.

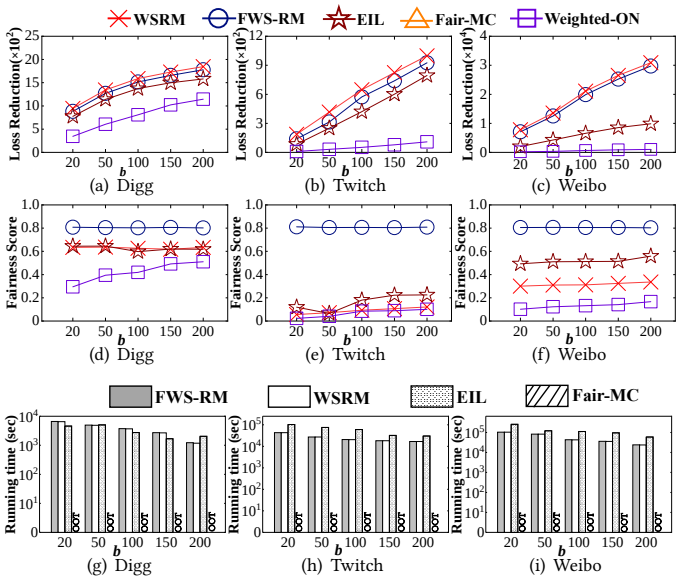

Figure 17: Reduction Losses / FS / Running Time vs. b (historical)

Varying the error factor ϵ. We study the impact of error factor on loss reduction, running time and fairness score by varying ϵ from 0.1 to 0.3. Since only FWS-RM, WSRM and EIL provide a theoretical guarantee, we show the result of these three algorithms. In Figure 18, 23-25, 32-34, it can be observed that as ϵ increases, the reduction loss decreases slightly, this is because when ϵ is small, the number of RR-Sets is of great largeness, the difference between the upper and lower bounds is smaller (in another words, the bounds are tighter and the results are closer to actual reward that with more loss reduction), thus the calculated value is larger. Meanwhile, an upswing of ϵ is linked with not just diminished implementation durations for all three algorithms, but also a gradual elevation in their respective fairness scores. It is worth claiming that FWS-RM significantly improves fairness, and through running time analysis, it can be found that meeting fairness does not bring a lot of time overhead. Another point worth mentioning is that TLRM problems often require shorter running times than RM problems. Although they both use the OPIM framework, TLRM often meets the accuracy requirements in fewer rounds because it generates fewer RR-Sets and takes less time to run, this accounts for the circumstances that FWS-RM usually runs faster than EIL. Last but not least, as shown in Figure 18(g), the EIL takes a shorter time in Digg. This underlying reason is that in Digg with historical set function, the weights of most users are very close to 1, thus the problem can be regarded as a more complex RM problem, therefore FWS-RM takes more time.

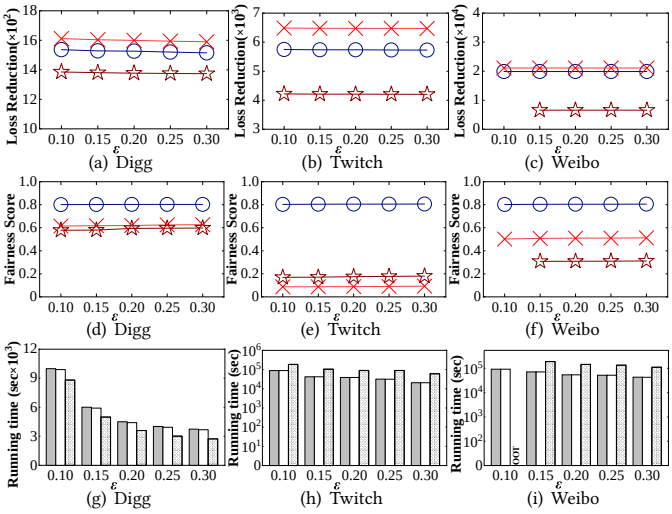

Figure 18: Reduction Losses / FS / Running Time vs. ϵ (historical)

Varying the α. Since only FWS-RM uses the fairness parameter α, we compare the loss reduction (i.e., effectiveness) and running time (i.e., efficiency) of FWS-RM by varying α which is displayed in Figure 19, 26, 35. Observations reveal that as α increases, loss reduction decreases within the range of 5%-9%, this suggests that FWS-RM can enhance the fairness of the algorithm at the cost of a slight reward reduction. Concurrently, a minor increase in running time is seen, attributed to the additional time required by the algorithm to comply with stricter fairness constraints.

Lower Bound. Figure 27 shows the lower bounds of β, which is the data-dependent approximation guarantee (Lemma 1) achieved by FWS-RM. It is easy to find that among all datasets $\beta > 0.6$, proving the tightness of our bound. Besides, we also compared our lower bound with the bound mentioned in Lemma 3, as show in Figure 28. Our tightness improved by about 5% on average, proving that our new bound has a better approximation effect.

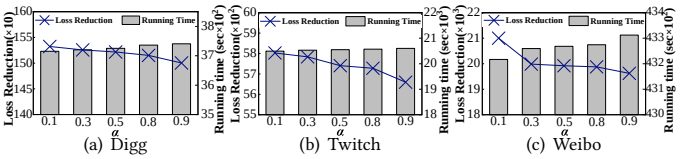

(a) Digg (b) Twitch (c) Weibo

Figure 19: Reduction Losses / Running Time vs. α (historical)

B PROOFS

B.1 DETAILED PROOF OF LEMMA 3

Lemma 4. *$\bar{r}_X(S_T \to v)$ under (9) is submodular.*

Proof. By applying truth-dominant policy r' and set all the MLs to 1 for campaign T will definitely increase the reward, therefore, it forms a upper bound. Since under (9), truth always dominates, thus the cases reduce to whether $a(\mathcal{P}_v^T, \mathcal{P}_v^F)$ equals to 0 or not.

Now fix a possible world X. For any node $v \in MAS_X$, when a node is added to S_T, v will either remain activated in F or switch to activating in T. To prove submodularity, it is sufficient to prove submodularity for each $v \in MAS_X$ due to the closed property of submodular functions [15]. Consider a truth set B and a node $w \in V \setminus (S_F \cup B)$:

Case(i): When $a(\mathcal{P}_v^T, \mathcal{P}_v^F) = 0$, the combination effect does not exist, therefore, $r'_X(S_T \to v) = max_{u \in S_T} r'_X(\{u\} \to v)$. If v is influenced by F under B, but influenced by T under $B \cup \{w\}$ w/o a tie-breaking, for v to satisfy Inequality 6, under B, $t_v^F < t_v^T$, and under $B \cup \{w\}$, $t_v^T < t_v^F$. Therefore, the shortest path from $B \cup \{w\}$ to v must begin with w; otherwise, it contradicts the condition. w contributes to the reward.

Case(ii): When $a(\mathcal{P}_v^T, \mathcal{P}_v^F) = 1$, by set all the MLs to 1 for campaign T, the node in S_T gain the same power like *combination effect* since the *combination effect* itself comes from the meeting delay of truth, this strength is further enhanced by truth-dominant policy. If a node v is influenced by F under B, but influenced by T under $B \cup \{w\}$ regardless of whether the truth-domination policy is used, for v to satisfy Inequality 6, it must be that under B, $t_v^F < t_v^T$, and under $B \cup \{w\}$, $t_v^T \le t_v^F$. Therefore, the shortest path from $B \cup \{w\}$ to v must begin with w; otherwise, it contradicts the condition. w also contributes to the reward.

From the above two cases, we could conclude that $\bar{r}_X(B \cup \{w\} \to v) = \bar{r}_X(\{w\} \to v)$. Let $A \subseteq B$, similar to the situation of B, we can get $\bar{r}_X(A \cup \{w\} \to v) = \bar{r}_X(\{w\} \to v) = \bar{r}_X(B \cup \{w\} \to v)$. Besides, the monotonicity of $\bar{r}$ implies that $\bar{r}_X(A \to v) \le \bar{r}_X(B \to v)$, therefore, $\bar{r}_X(A \cup \{w\} \to v) - \bar{r}_X(A \to v) \ge \bar{r}_X(B \cup \{w\} \to v) - \bar{r}_X(B \to v)$, the proof ends. □

B.2 DETAILED PROOFS OF THE UNBIASED ESTIMATE $\mathbb{R}(S_T)$

Conclusion. $\mathbb{R}(S_T) = INF \cdot \mathbb{E}[Y(S_T, R)]$

Proof. Let $\Pr_X(S_F \to v)$ represent the probability that v is affected by S_F in a possible world X, and $\Pr_X(S_T \to v = w(v))$ indicates the probability that S_T can propagate to v before S_F, or that v believes the truth through tie-breaking in a possible world X. When the root v of R_i is selected uniformly at random from MAS_X:

$$\begin{aligned}
\mathbb{R}(S_T) &= \sum_v [Pr_X(S_F \to v) \cdot Pr_X(S_T \to v = w(v))] \\
&= \sum_v [Pr_X(S_F \to v) \cdot Pr_X(S_T \cap R_i(v) = w(v))] \\
&= \sum_v Pr_X(S_F \to v) \cdot [Pr_X(S_T \cap R_i(v) = w(v))] \\
&= INF \cdot [Pr_X(S_T \cap R_i(v) = w(v))] \\
&= INF \cdot \mathbb{E}[Y(S_T, R)]
\end{aligned}$$

□

B.3 PROOFS ABOUT TIME COMPLEXITY

Conclusion. The time complexity of FWS-RM is $O(\sum_{R \in \mathcal{R}_1 \cup \mathcal{R}_2} (INF_F + \frac{m}{n} \cdot (INF_1)^2)$, where INF_F is the influence spread of S_F and INF_1 is the largest reverse expected influence spread of any size-one node set in G.

Proof. Since the main time cost of the FWS-RM comes from the generation of RR-Sets, we can get the algorithm time complexity of FWS-RM is $O(\sum_{R \in \mathcal{R}_1 \cup \mathcal{R}_2} EPT)$, where EPT is the expected complexity of generating a RR-Set. During the generation process of RR-Sets, we first perform BFS of the S_F, the time complexity of which is INF_F. Then we did a reverse Dijkstra, it has a running time of $n^* log n^* + m^*$, where n^* and m^* are the number of nodes and edges inspected by the randomly chosen node, solving the tie-breaking need a time cost of $n^* m^*$. Therefore, the EPT can be calculated as follows:

$$EPT = INF_F + \mathbb{E}[n^* log n^* + m^* + n^* m^*]$$

The size of n^* is bounded by INF_1 due to the fact that INF_1 is the largest reverse expected influence spread of the a node r in G, using the conclusion from [51], we can get $m^* \le \frac{m}{n} INF_1$. Combining all the above conclusions, we can get

$$\begin{aligned}
EPT &= INF_F + \mathbb{E}[n^* \log n^* + m^* + n^* m^*] \\
&\le INF_F + \mathbb{E}[2 \cdot n^* m^*] \\
&= O(INF_F + \frac{m}{n} \cdot (INF_1)^2)
\end{aligned}$$

Thus, the time complexity of FWS-RM is $O(\sum_{R \in \mathcal{R}_1 \cup \mathcal{R}_2} (INF_F + \frac{m}{n} \cdot (INF_1)^2)$, the proof ends. □

C DETAILED EXPERIMENT ABOUT CHARACTERISTICS OF BETTER-PERFORMING SOCIAL NETWORKS

Table 7: Metric of the group that has the greatest impact on loss reduction in LastFM and Facebook.

Metric \ Datasets	LastFM	Facebook
In-degree	6.9 (The second least)	8.8 (The least)
Out-degree	7.5 (The least)	9.2 (The second least)
Rumor reach probability	0.459	0.411

As show in 7, both the rank of In-degree, Out-degree and Rumor reach probability in the worst performance group are the last or the second last, and there are minor differences between them comparing with Harmonic Centrality, emphasizing the importance of Harmonic Centrality in good algorithm-performing.

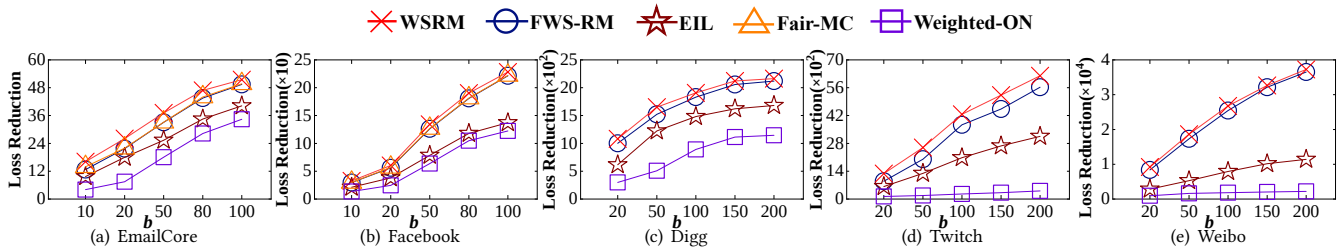

Figure 20: Reduction Losses vs. b (topology)

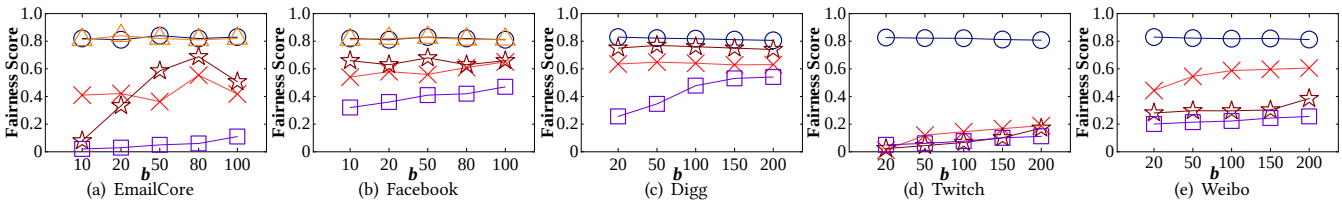

Figure 21: Fairness Score vs. b (topology)

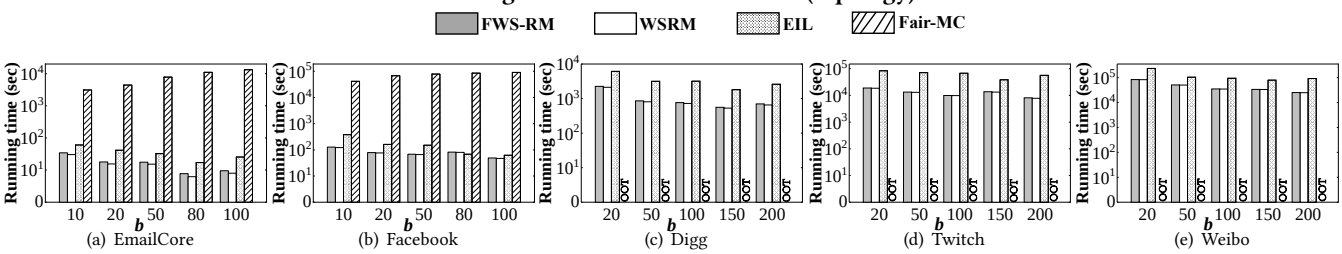

Figure 22: Running time vs. b (topology)

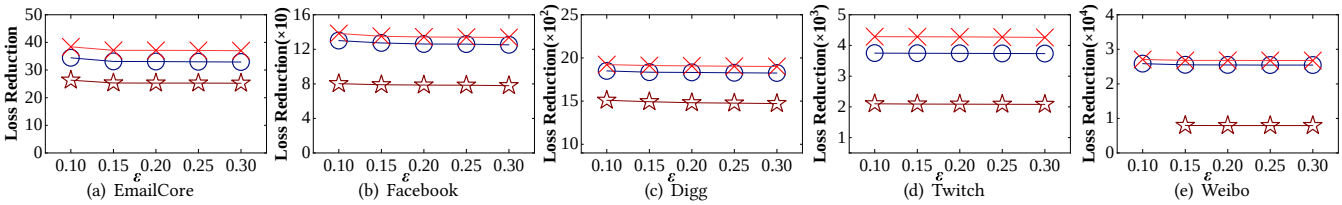

Figure 23: Reduction Losses vs. ϵ (topology)

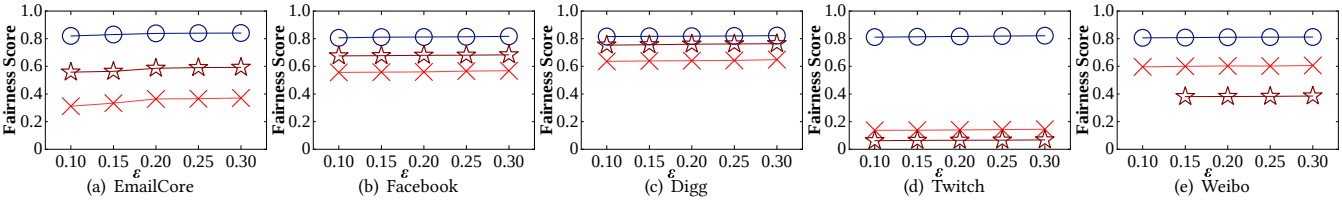

Figure 24: Fairness Score vs. ϵ (topology)

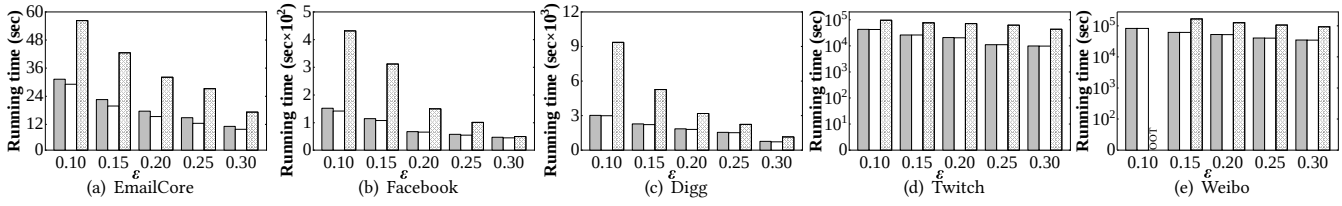

Figure 25: Running time vs. ϵ (topology)

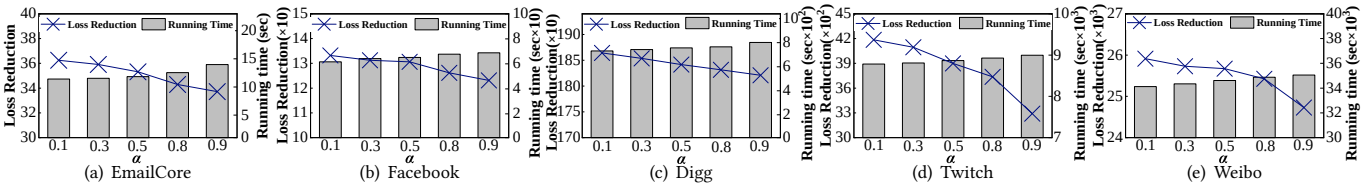

Figure 26: The impact of α on loss reduction and running time (topology)

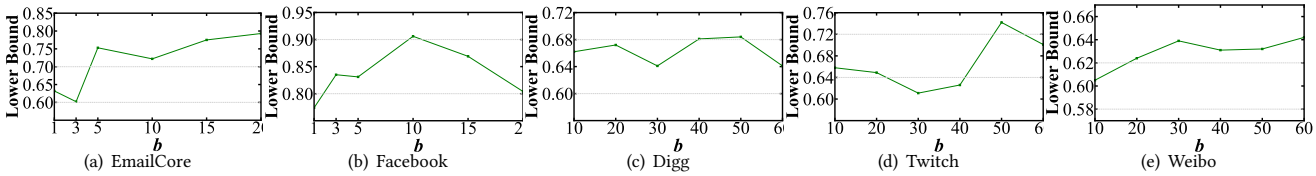

Figure 27: The lower bound of β (tightened)

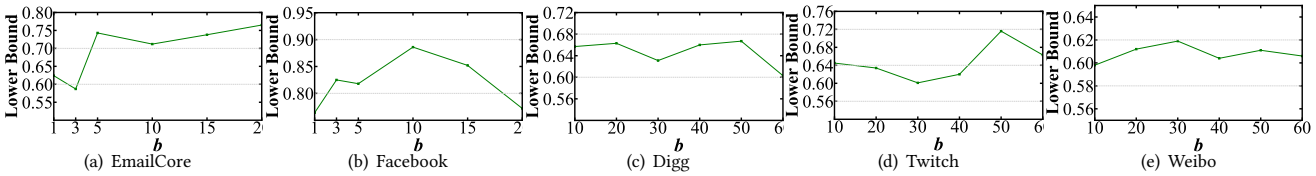

Figure 28: The lower bound of β (ordinary)

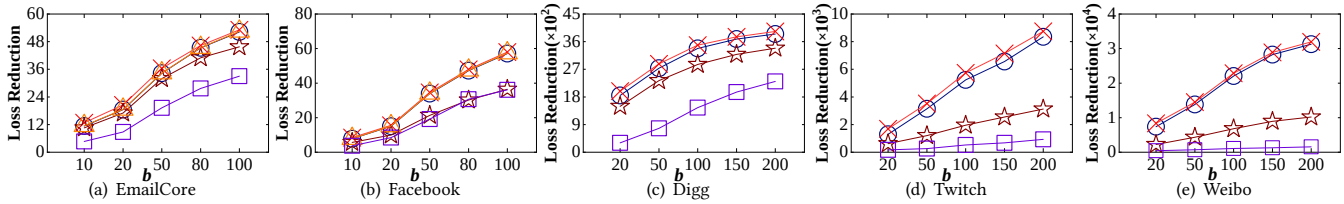

Figure 29: Reduction Losses vs. b (random)

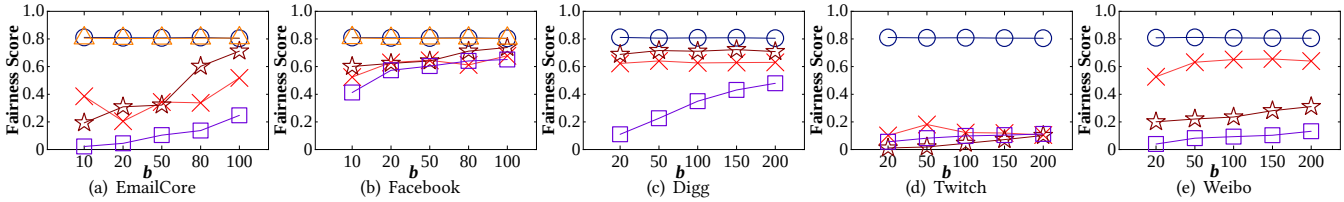

Figure 30: Fairness Score vs. b (random)

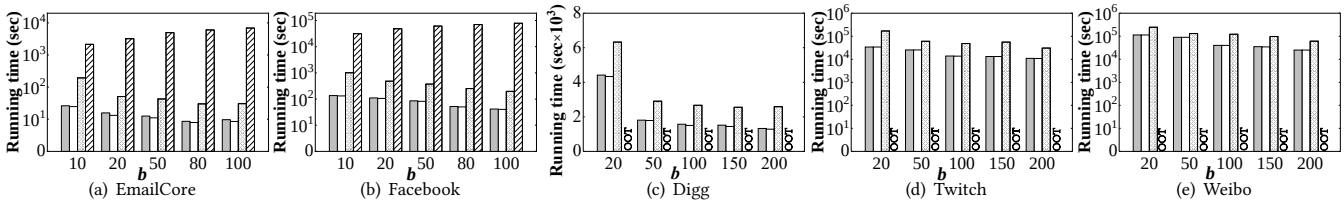

Figure 31: Running time vs. b (random)

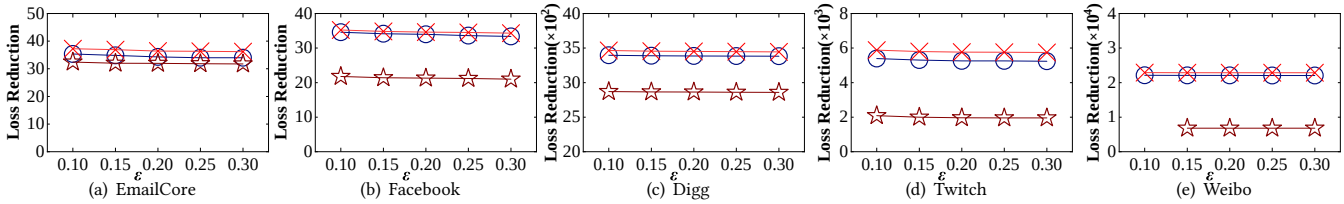

Figure 32: Reduction Losses vs. ϵ (random)

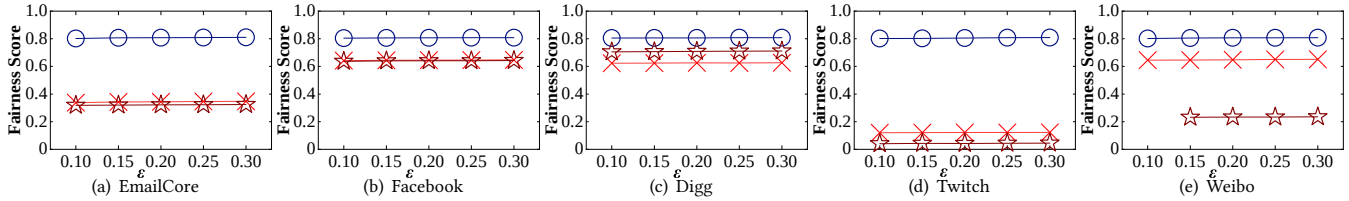

Figure 33: Fairness Score vs. ϵ (random)

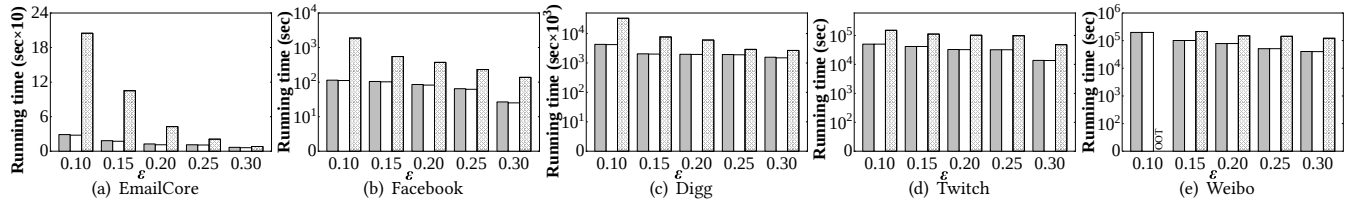

Figure 34: Running time vs. ϵ (random)

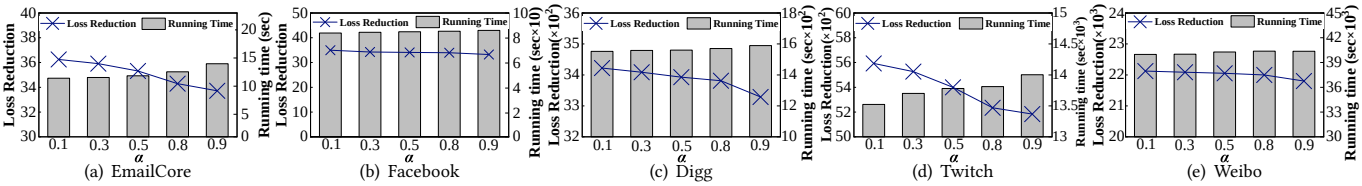

Figure 35: The impact of α on loss reduction and running time (random)